AGU PUBLICATIONS

Geochemistry, Geophysics, Geosystems

RESEARCH ARTICLE

10.1002/2016GC006400

Key Points:
- Late-Pleistocene precipitation was ^{18}O-depleted relative to the late-Holocene over the great majority of the global landmass
- Late-Pleistocene precipitation was ^{18}O-enriched throughout much of southeastern Asia and close to some coastlines
- Fossil groundwater δ^{18}O maps may help to test ideas about mammal movements, glacial climates, and groundwater ages

Supporting Information:
- Supporting Information S1

Correspondence to:
S. Jasechko,
sjasechk@ucalgary.ca

Citation:
Jasechko, S. (2016), Late-Pleistocene precipitation δ^{18}O interpolated across the global landmass, *Geochem. Geophys. Geosyst.*, *17*, 3274–3288, doi:10.1002/2016GC006400.

Received 13 APR 2016
Accepted 9 JUL 2016
Accepted article online 13 JUL 2016
Published online 16 AUG 2016

Late-Pleistocene precipitation δ^{18}O interpolated across the global landmass

Scott Jasechko[1]

[1]Department of Geography, University of Calgary, Calgary, Alberta, Canada

Abstract Global water cycles, ecosystem assemblages, and weathering rates were impacted by the ~4°C of global warming that took place over the course of the last glacial termination. Fossil groundwaters can be useful indicators of late-Pleistocene precipitation isotope compositions, which, in turn, can help to test hypotheses about the drivers and impacts of glacial-interglacial climate changes. Here, a global catalog of 126 fossil groundwater records is used to interpolate late-Pleistocene precipitation δ^{18}O across the global landmass. The interpolated data show that extratropical late-Pleistocene terrestrial precipitation was near uniformly depleted in ^{18}O relative to the late Holocene. By contrast, tropical δ^{18}O responses to deglacial warming diverged; late-Pleistocene δ^{18}O was higher-than-modern across India and South China but lower-than-modern throughout much of northern and southern Africa. Groundwaters that recharged beneath large northern hemisphere ice sheets have different Holocene-Pleistocene δ^{18}O relationships than paleowaters that recharged subaerially, potentially aiding reconstructions of englacial transport in paleo ice sheets. Global terrestrial late-Pleistocene precipitation δ^{18}O maps may help to determine 3-D groundwater age distributions, constrain Pleistocene mammal movements, and better understand glacial climate dynamics.

1. Introduction

Deglacial changes to atmospheric temperatures and water fluxes between the late-Pleistocene (~20000-50,000 years ago) and the late-Holocene (within the last ~5000 years) increased global sea levels, melted two large northern hemisphere ice sheets, and rearranged terrestrial biomes [*Clark et al.*, 2009; *Williams*, 2009]. Late-Pleistocene precipitation isotope (δ^{18}O) records are applied widely to understand the impacts of deglacial climate warming on earth systems and to better understand groundwater renewal rates (e.g., ice core, speleothem and groundwater records [*Thompson et al.*, 1989; *Bar-Matthews et al.*, 1997; *Edmunds*, 2009]; where $\delta^{18}O = ([^{18}O/^{16}O_{\text{sample}}]/[^{18}O/^{16}O_{\text{Vienna standard mean ocean water}}] - 1)\times 10^3$ ‰). A key limitation of some paleoclimate evaluations are regional absences of measurement-based constraints on glacial climate conditions [*Harrison et al.*, 2015].

One type of Pleistocene precipitation δ^{18}O record that has been widely identified and explored are the fossil groundwaters that recharged during the Pleistocene, replenished either by the direct infiltration of precipitation, by focused recharge beneath rivers or lakes, or by the influx of pressurized subglacial meltwaters that existed beneath large northern hemisphere ice sheets during the last ice age [e.g., *Edmunds and Wright*, 1979; *Phillips et al.*, 1986; *Rozanski*, 1985; *Stute and Deák*, 1989; *Remenda et al.*, 1994; *Aeschbach-Hertig et al.*, 2002; *Edmunds*, 2009; *Taylor et al.*, 2013a]. Interpreting climate signals from fossil groundwater δ^{18}O records requires understanding processes that govern modern groundwater δ^{18}O values. Modern groundwater δ^{18}O values integrate a suite of processes that take place as the water vapor travels inland, condenses, falls, and flows to a location in the aquifer [*Dansgaard*, 1964; *Gat*, 1996]. Some of the processes impacting modern meteoric δ^{18}O values include physiochemical conditions at the ocean-atmosphere interface during evaporation at the moisture origin, upwind precipitation-evapotranspiration balances and air mass mixing, seasonal variability in precipitation fluxes, seasonal or interannual variations in the ratio of groundwater recharge as a proportion of precipitation, postdepositional isotope effects, and mixing of waters in the aquifer or soil profile [*Vogel et al.*, 1963; *Simpson et al.*, 1972; *Salati et al.*, 1979; *Rozanski et al.*, 1993 ; *Feng et al.*, 2009; *Risi et al.*, 2013; *Winnick et al.*, 2014]. It is therefore possible that deglacial δ^{18}O shifts recorded in fossil groundwaters capture information about the shifts to these and other hydrogeochemical processes that were brought about by the natural climate changes that took place between the late-Pleistocene and the late-Holocene.

Efforts to identify leading drivers of past precipitation δ^{18}O shifts often benefit from exploring multiple records in a region [*Pausata et al*., 2011; *Mix and Chamberlain*, 2014]. Further, several isotope-enabled general circulation models now exist and have been analyzed under recent and glacial climate states [e.g., *Lee et al*., 2009]. Combining global glacial climate simulations and measured late-Pleistocene precipitation δ^{18}O records could help to test ideas about deglacial climate changes. However, a measurement-driven map of late-Pleistocene precipitation δ^{18}O across the global landmass remains unavailable.

The objective of this study is to map changes to global terrestrial precipitation δ^{18}O between the late-Pleistocene and the late-Holocene across the global landmass. This analysis builds on two recent compilations of the isotopic compositions of fossil groundwaters recharged subaerially or subglacially [*Jasechko et al*., 2015; *Ferguson and Jasechko*, 2015]. This analysis differs from each of these two previous works in a number of ways, two of which include the analysis of a substantially greater number of isotope records than have been analyzed previously ($\sim$twice as many), and the development of the first measurement-driven estimate of late-Holocene/late-Pleistocene precipitation δ^{18}O shifts that spans across the global landmass. Critically, the much larger number of records analyzed here is sufficient to interpolate late-Pleistocene precipitation δ^{18}O values around much of the globe, which was not achievable using smaller data sets [*Jasechko et al*., 2015]. Herein, the difference between late-Pleistocene precipitation δ^{18}O and late-Holocene δ^{18}O is defined as: $\Delta^{18}\mathrm{O}_{\text{late-Pleistocene}} = \delta^{18}\mathrm{O}_{\text{late-Pleistocene}} - \delta^{18}\mathrm{O}_{\text{late-Holocene}}$.

2. Approach

2.1. Calculating Late-Pleistocene Precipitation δ^{18}O

Deglacial precipitation δ^{18}O shifts were calculated for 154 proxy records compiled from the primary literature and specialist databases (supporting information; Figure 1). Fossil groundwaters constitute the great majority (82%) of the synthesized records; the other records explored here are speleothems and ice cores. This study interprets isotope compositions of groundwater samples that have radiocarbon dates exceeding 20,000 years as approximations of late-Pleistocene precipitation δ^{18}O (see section 2.3 entitled Calculation Limitations).

This study compares measured oxygen isotope compositions of paleoclimate records analyzed over two time intervals: the late-Holocene represented by the past 5000 calendar years ($\delta^{18}\mathrm{O}_{\text{late-Holocene}}$), and the late-Pleistocene represented by $\sim$20,000 to $\sim$50,000 calendar years before present ($\delta^{18}\mathrm{O}_{\text{late-Pleistocene}}$). The relatively coarse temporal resolutions of each time interval are necessary in order to interpret the groundwater records, which are characterized by uncertain ^{14}C-based ages ($\pm$1000s of years). These boundaries set for the late-Holocene and late-Pleistocene are approximate and are defined by the uncertainty margins and practical limits of radiocarbon-based groundwater age dating.

Groundwater ages were determined using measured ^{3}H and ^{14}C radioactivities, correcting the ages determined from the latter on the basis of measured ^{13}C/^{12}C ratios [*Clark and Fritz*, 1997] (see methods in *Jasechko et al*., 2015]. Once an estimated age for each sample was calculated, δ^{18}O shifts between the late-Pleistocene and the late-Holocene ($\Delta^{18}\mathrm{O}_{\text{late-Pleistocene}}$) were determined by the difference between $\delta^{18}\mathrm{O}_{\text{late-Pleistocene}}$ and $\delta^{18}\mathrm{O}_{\text{late-Holocene}}$ (errors determined following Gaussian error propagation).

To complement the fossil ground records, a series of ice core and cave calcite records are also analyzed here. Cave calcite $\Delta^{18}\mathrm{O}_{\text{late-Pleistocene}}$ records have been corrected for the different temperatures prevailing during the late-Holocene and late-Pleistocene time periods that likely impacted H_2O-$CaCO_3^{18}O$ fractionation factors [*Jasechko et al*., 2015] (temperature-fractionation equation from *O'Neil et al*., 1969]. Temperatures used to correct speleothem data for temperature changes were estimated using last glacial maximum [*Annan and Hargreaves*, 2013] and modern [*New et al*., 2002] temperature estimates. Therefore, the method used to correct speleothem records for temperature effects introduces additional sources of uncertainty, because the speleothem records were analyzed over a timeframe ($\sim$20–50 ka) that overlaps only in part with the Last Glacial Maximum ($\sim$19-23 ka), and because modern temperatures are imperfect approximations of late-Holocene temperatures [*Marcott et al*., 2013]. However, this additional uncertainty, which impacts only the speleothem records, is expected to be less than $\sim$0.5‰. An arguably more important uncertainty lies in the averaging of speleothem data over the necessarily coarse late-Holocene and late-Pleistocene time intervals.

Reports of subglacial groundwater recharge from large, northern hemisphere ice sheets rarely include ^{14}C measurements. In order to include these data in this synthesis, $\Delta^{18}O_{\text{late-Pleistocene}}$ values for subglacial recharge archives were calculated using the minimum measured groundwater $\delta^{18}O$ value as an estimate of the subglacial recharge endmember (i.e., $\delta^{18}O_{\text{late-Pleistocene}}$) [*Ferguson and Jasechko*, 2015]. First, nearby (~100 km) subglacial recharge data sets were combined. Next, $\delta^{18}O_{\text{late-Holocene}}$ values for each subglacial recharge record were estimated using interpolated modern precipitation $\delta^{18}O$ values [*Bowen and Wilkinson*, 2002]. This data analysis approach applied to subglacial groundwater records introduces several potential biases because modern precipitation $\delta^{18}O$ likely differs from late-Holocene precipitation, because global precipitation $\delta^{18}O$ often differs from modern groundwater $\delta^{18}O$ [*Vogel et al.*, 1963; *Simpson et al.*, 1972], because the lowest $\delta^{18}O$ value in a regional aquifer may not represent the absolute glacial end-member $\delta^{18}O$ value due to mixing with more recent waters, and because paleo ice sheet isotope compositions likely varied throughout the last ice age and the timing of subglacial recharge remains unclear for most samples. Due to these potential biases, subglacial groundwater isotope records are discussed separately from the other groundwater records that capture direct, subaerial recharge; further, subglacial recharge records are excluded from the geospatial analysis described in the following section 2.2.

2.2. Mapping Late-Pleistocene $\delta^{18}O$

The spatial variability of late-Holocene and late-Pleistocene $\delta^{18}O$ values was estimated following an approach developed for modern precipitation $\delta^{18}O$ [*Bowen and Wilkinson*, 2002]. First, records located within 200 m of sea level were separated from records located at higher altitudes. These low elevation $\delta^{18}O$ records were used to develop second-order regressions of $\delta^{18}O$ and the absolute value of latitude (|Lat|) for the late-Holocene (equation (1)) and the late-Pleistocene (equation (2)):

$$\delta^{18}O_{\text{late-Holocene}} = -0.006566(|\text{Lat}|)^2 + 0.2897(|\text{Lat}|) - 7.5 \quad [R^2 = 0.66] \tag{1}$$

$$\delta^{18}O_{\text{late-Pleistocene}} = -0.008467(|\text{Lat}|)^2 + 0.3828(|\text{Lat}|) - 8.8 \quad [R^2 = 0.65] \tag{2}$$

Only groundwater and glacial ice records were used to develop equations (1) and (2); cave calcite records were not used because they record relative shifts in $\delta^{18}O$ rather than absolute values. $\delta^{18}O$ records located more than 200 m above sea level tend to be depleted in ^{18}O relative to $\delta^{18}O$ values predicted using equations (1) and (2). The magnitude of deviation between predicted versus measured $\delta^{18}O$ values increases with altitude. An empirical "altitude effect" was determined by regression analysis of altitude versus the $\delta^{18}O$ deviation (where [$\delta^{18}O$ deviation] = [measured $\delta^{18}O$ for the late-Holocene or late-Pleistocene] – [predicted $\delta^{18}O$ from equation (1) or (2)]). Empirical "altitude effects" were estimated to be $-3.3‰\ km^{-1}$ for the late-Holocene ($R^2 = 0.50$) and $-3.8‰\ km^{-1}$ for the late-Pleistocene ($R^2 = 0.54$).

Predictions of groundwater $\delta^{18}O$ for the late-Holocene and the late-Pleistocene were determined by combining the two regressions describing the empirical relationships of latitude, altitude, and $\delta^{18}O$ [*Bowen and Wilkinson*, 2002]:

$$\delta^{18}O_{\text{late-Holocene}} = -0.006566(|\text{Lat}|)^2 + 0.2897(|\text{Lat}|) - 3.3(Alt) - 7.5 \tag{3}$$

$$\delta^{18}O_{\text{late-Pleistocene}} = -0.008467(|\text{Lat}|)^2 + 0.3828(|\text{Lat}|) - 3.8(Alt) - 8.8 \tag{4}$$

where *(Alt)* represents the elevation of the isotopic record above sea level (in kilometers).

Equations (3) and (4) were used to estimate $\delta^{18}O$ changes from the late-Pleistocene to the late-Holocene. Next, residuals were calculated for each isotope record by comparing predicted (i.e., results of equations (3) and (4)) and measured proxy record isotope compositions. Residuals were interpolated (inverse distance weighted) and applied as a correction factor to global grids developed from equations (3) and (4). Cave calcite records, while excluded from the development of equations (1–4), were applied in the residual correction step.

2.3. Calculation Limitations

This global and measurement-driven map of late-Pleistocene to late-Holocene precipitation $\delta^{18}O$ shifts is complicated by a number of uncertainties.

First, calculated groundwater radiocarbon age dates implicitly assume that substantial mixing of young and old groundwaters does not take place in the aquifer or along the drilled well; neither assumption is likely valid for all collected samples [*Torgersen et al*., 2013]. This study uses a straightforward, widely applied, carbon-isotope-based approach to estimate the "mean" groundwater age of each individual sample [*Clark and Fritz*, 1997]. This method is vulnerable to aggregation errors when the groundwater sample contains a mixture of recent recharge and Pleistocene paleowater [*Jasechko*, 2016], potentially leading to differences between calculated and true $\Delta^{18}O_{\text{late-Pleistocene}}$ values. In an effort to reduce impacts of this known aggregation bias, the lower-limit of the late-Pleistocene time interval was set higher (~20,000 years ago) than the Pleistocene-Holocene boundary (11,700 years ago), which may be a more logical lower-limit [e.g., *Turney et al*., 2015]. For most sampled groundwater systems, the $\delta^{18}O$ values level off for samples with ages exceeding ~20,000 years (see supporting information Figures S1–S57 in *Jasechko et al*. [2015]). In addition, ^{14}C-based groundwater dating techniques cannot distinguish groundwaters that recharged ~50,000 years ago from much older waters that may predate the Pleistocene [*Torgersen et al*., 2013]. The possibility that a fraction of a groundwater sample which has a calculated mean age falling within the ascribed late-Pleistocene time interval of ~20–50 thousand years is, in fact, considerably older than ~50 thousand years, cannot be ruled out [e.g., *Patterson et al*., 2005; *Kulongoski et al*. 2008].

Second, groundwater and speleothem $\delta^{18}O$ records are interpreted to represent precipitation $\delta^{18}O$ values; however, in some regions, the $\delta^{18}O$ of infiltration differs from the annual precipitation $\delta^{18}O$ value. Precipitation-groundwater comparisons show that recent recharge is often ^{18}O-depleted relative to annual amount-weighted precipitation isotope compositions due to the seasonal bias in the groundwater recharge ratio to winter precipitation and intensive rainfall [e.g., *Vogel et al*., 1963; *Simpson et al*., 1972; *Airey et al*., 1980; *Grabczak et al*., 1984; *Maulé et al*., 1994; *Winograd et al*., 1998; *Abbott et al*., 2000; *Jones and Banner*, 2003; *O'driscoll et al*., 2005; *Florea*, 2013; *Jasechko et al*., 2014; *Jasechko and Taylor*, 2015; *Sánchez-Murillo and Birkel*, 2016]. It is therefore possible that changes to the degree of seasonal bias in the groundwater recharge ratio between the late-Holocene and the late-Pleistocene influence $\Delta^{18}O_{\text{late-Pleistocene}}$ values recorded by groundwater and speleothem records.

Third, the time interval that has been ascribed to the late-Pleistocene (20–50 thousand years ago) includes numerous and substantial climate changes that are amalgamated, likely unevenly, in the $\Delta^{18}O_{\text{late-Pleistocene}}$ values calculated here. For example, this ascribed late-Pleistocene time interval spans 12 Dansgaard/Oeschger Events (2–13, inclusive), covers four Heinrich Events (H2–H5, inclusive), and poorly captures the timing of minima and maxima of well-established, millennial-scale $\delta^{18}O$ cycles found in some regions [*Dansgaard et al*., 1993; *Grootes and Stuiver*, 1997; *Wang et al*., 2007; *Turney et al*., 2015]. Further, it is unlikely that $\Delta^{18}O_{\text{late-Pleistocene}}$ records capture precipitation $\delta^{18}O$ shifts over the course of the ascribed late-Holocene and late-Pleistocene time periods evenly. For example, fossil groundwater records in the tropics are likely to disproportionately represent pluvial time periods when groundwater recharge ratios (recharge/precipitation) are maximized [*Taylor et al*., 2013b; *Jasechko and Taylor*, 2015]. Further complications may arise near to river corridors where the possibility that groundwaters were recharged beneath riverbeds by precipitation that fell at higher altitudes cannot be dismissed [e.g., *Datta et al*., 1996]. The uneven sampling of amount-weighted, annual precipitation $\delta^{18}O$ by the proxy records likely impacts calculated $\Delta^{18}O_{\text{late-Pleistocene}}$ values presented here. However, by analyzing precipitation $\delta^{18}O$ records over the late-Holocene and late-Pleistocene time periods at coarser time-scales, an analysis of a large data set of fossil groundwater $\delta^{18}O$ records becomes possible, permitting an examination of how precipitation $\delta^{18}O$ values shifted as global climate shifted from cooler (~20–50 ka) to warmer (~0–5 ka) conditions.

A fourth assumption implicit in this analysis is that groundwater, speleothem, and ice core records preserve the primary $\delta^{18}O$ value of meteoric water. However, there are a number of hydrogeochemical processes that can impact $\delta^{18}O$ values during or following the preservation of these isotope records. Groundwater $\delta^{18}O$ records may be impacted by postrecharge processes such as partial evaporation, groundwater mixing, high-temperature water rock interactions, and other hydrogeochemical processes [*Cartwright et al*., 2012]. Efforts were made to minimize the possibility of substantial influence of these effects on the calculated $\Delta^{18}O_{\text{late-Pleistocene}}$ values by excluding samples reported to possibly be impacted by substantial geothermal activity or seawater intrusion [e.g., *Morrissey et al*., 2010]. Speleothem records may not capture annual precipitation isotope compositions due to evaporative cooling of cave drip waters [*Cuthbert et al*., 2014] or disequilibrium conditions imparted by seasonal differences in drip water fluxes [*Mickler et al*., 2006; *Deininger*

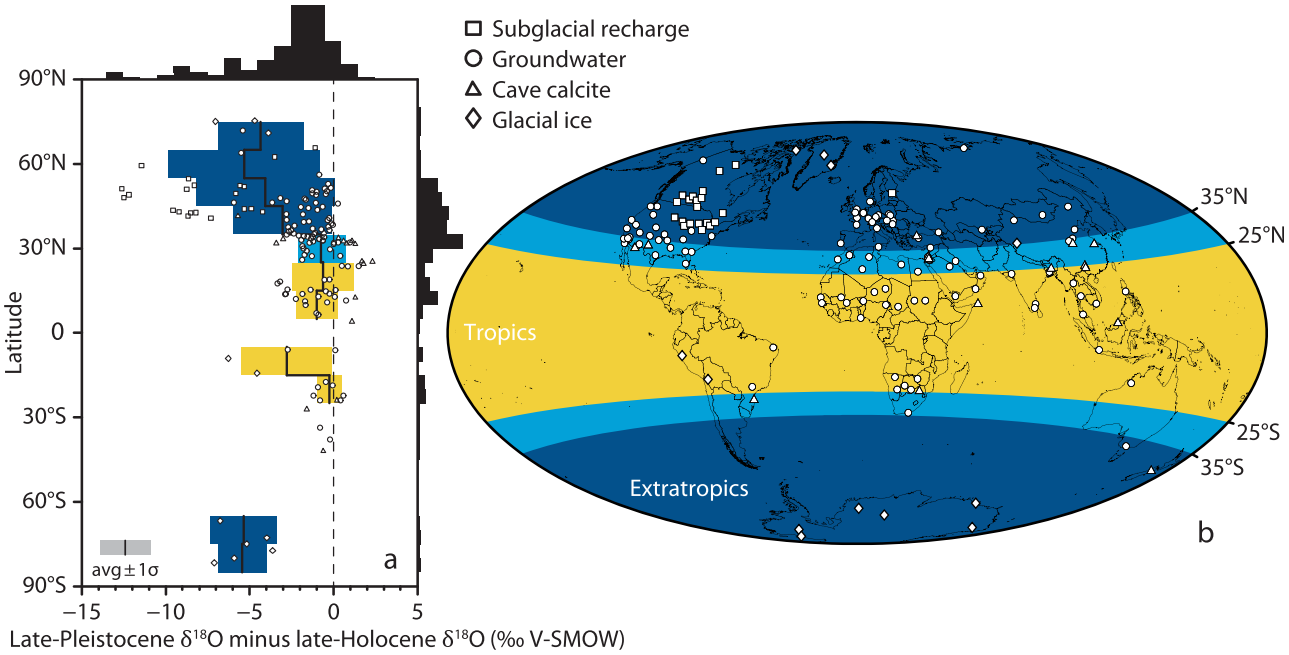

Figure 1. Late-Pleistocene precipitation δ^{18}O records (n = 154). (a) The latitudinal distribution of $\Delta^{18}O_{\text{late-Pleistocene}}$ values for subglacial recharge (squares), groundwater (circles), cave calcite (triangles), and glacial ice (diamonds; $\Delta^{18}O_{\text{late-Pleistocene}} = \delta^{18}O_{\text{late-Pleistocene}} - \delta^{18}O_{\text{late-Holocene}}$). The average $\Delta^{18}O_{\text{late-Pleistocene}}$ ($\pm$1 standard deviation) is delineated as bars along 10° latitudinal bins. Histograms are shown along the upper and right-side borders. (b) The locations of the records, and delineates the approximate boundaries of the tropics (yellow), subtropics (light blue), and extratropics (dark blue). Primary data sets were cataloged from International Atomic Energy Agency and U. S. Geological Survey databases, and from the primary literature. The International Atomic Energy Agency TWIN database was downloaded from dev.geo.univie.ac.at/projects/wiser/twin.php. The U. S. Geological Survey database was downloaded from the database available at www.waterqualitydata.us (both databases were accessed in November 2014). Primary literature data sources from which data were compiled include *Aeschbach-Hertig et al.* [2002]; *Aggarwal et al.* [2000]; *Al-Mashaikhi et al.* [2012]; *Al-Ruwaih and Shehata* [2004]; *Andrews et al.* [1994]; *Aravena and Wassenaar* [1993]; *Asmerom et al.* [2010]; *Bar-Matthews et al.* [2003]; *Barbecot et al.* [2000]; *Berkelhammer et al.* [2012]; *Beyerle et al.* [1998, 2003]; *Blunier and Brook* [2001]; *Brown et al.* [2011]; *Buiron et al.* [2011]; *Cai et al.* [2010]; *Castany et al.* [1974]; *Celle-Jeanton et al.* [2009]; *Chen et al.* [2005, 2011]; *Cheung and Mayer* [2009]; *Clark et al.* [1987, 1997, 1998, 2000]; *Cody et al.* [1999]; *Cruz et al.* [2005]; [*Currell et al.* [2010]; *Currell et al.* [2013]; *Darling et al.* [1997]; *Derwich et al.* [2012]; *Dodo and Zuppi* [1997, 1999]; *Douglas et al.* [2007]; *Dutt et al.* [2015]; *Dutton* [1995]; *Dykoski et al.* [2005]; *Eberts and George* [2000]; *Edmunds et al.* [2004] ; *Edmunds* [2009]; *Edmunds et al.* [2003]; *Elliot et al.* [1999]; *EPICA Community* [2006]; *Fadlelmawla et al.* [2008]; *Ferguson et al.* [2007]; *Fernandes and Carreira* [2008]; *Ferronsky et al.* [1991]; *Fleitmann et al.* [2009]; *Frumkin et al.* [1999]; *Gat and Galai* [1982]; *Geyh and Sofner* [1989]; *Geyh and Sofner* [1989]; *Gonfiantini et al.* [1974]; *Goni* [2006]; *Gosselin et al.* [2004]; *Gouvea da Silva* [1983]; *Grasby and Betcher* [2002]; *Grasby and Chen* [2005]; *Grasby et al.* [2003]; *Greene et al.* [2008]; *Hackley et al.* [2010]; *Hagedorn* [2015]; *Harrington et al.* [2011]; *Heaton et al.* [1986]; *Hendry and Wassenaar* [2009]; *Hendry et al.* [2013]; *Hinsby et al.* [2001]; *Hoaglund et al.* [2004]; *Holmgren et al.* [2003]; *Hoque and Burgess* [2012]; *Huneau et al.* [2011]; *Karro et al.* [2004]; *Kawamura et al.* [2007]; *Klump et al.* [2008]; *Kolak et al.* [1999]; *Kotler and Burn* [2000]; *Kreuzer et al.* [2009]; *Külls* [2000]; *Kulongoski et al.* [2004]; *Kumar et al.* [2009]; *Larsen et al.* [2002]; *Le Gal La Salle et al.* [1995, 2001]; *Li et al.* [2015]; *Majumder et al.* [2011]; *Martinelli et al.* [2014]; *Mazor et al.* [1995]; *McMahon et al.* [2004]; *Mehta et al.* [2000]; *Melikadze et al.* [2014]; *Meyer et al.* [2002]; *Naus et al.* [2001]; *Noseck et al.* [2009]; *Partin et al.* [2007]; *Patterson et al.* [1977, 2005]; *Pedro et al.* [2011]; *Person et al.* [2007]; *Phillips et al.* [1986]; *Rahube* [2003]; *Raidla et al.* [2009, 2012]; *Remenda et al.* [1994, 1996]; *Salati et al.* [1974]; *Samborska et al.* [2012]; *Schlegel et al.* [2009]; *Schwartz and Muehlenbachs* [1979]; *Shakun et al.* [2007]; *Shehata and Al-Ruwaih* [1999]; *Siegel and Mandle* [1984]; *Sikdar and Sahu* [2009]; *Stadler et al.* [2012]; *Stotler et al.* [2009, 2010]; *Stute and Deák* [1989]; *Sukhija et al.* [1998]; *Sultan et al.* [2007]; *Tenu et al.* [1975]; *Thompson et al.* [1995, 1997, 1998]; *van Geldern et al.* [2014]; *Varsányi et al.* [2011]; *Vinther et al.* [2006, 2008]; von *Rohden et al.* [2010]; *Wagner et al.* [2010]; *Walraevens* [1990]; *Wang et al.* [2001, 2007]; *Weaver et al.* [1995]; *Weyhenmeyer et al.* [2000, 2002]; *Wieser et al.* [2011]; *Williams et al.* [2010]; *Yang et al.* [2010]; *Yechieli et al.* [2008]; *Yuan et al.* [2004]; and *Zuber et al.* [2004].

et al., 2012]. Ice core records may be impacted by ice-vapor exchanges that can modify the δ^{18}O values that were ultimately preserved in the ice [*Steen-Larsen et al.*, 2014].

Simultaneous compilation and analysis of groundwater, speleothem and ice core records introduces several key uncertainties, some of which are discussed above. Therefore, the maps created in this study constitute nondefinitive estimates of world $\Delta^{18}O_{\text{late-Pleistocene}}$ distributions. Nevertheless, no other type of paleoclimate record has been identified and measured with such high-frequency across the global landmass as fossil groundwaters. The strong spatial coherence of calculated $\Delta^{18}O_{\text{late-Pleistocene}}$ values presented in section 3 indicates strongly that fossil groundwaters do indeed capture and preserve useful information about late-Pleistocene to late-Holocene precipitation δ^{18}O shifts. Keeping in mind the processes described above, this global catalog of $\Delta^{18}O_{\text{late-Pleistocene}}$ data represents the first measurement-driven estimate of deglacial shifts to global land precipitation δ_{18}O.

3. Results and Discussion

Geographic patterns of late-Pleistocene and late-Holocene precipitation δ^{18}O shifts are observed at both global and regional scales.

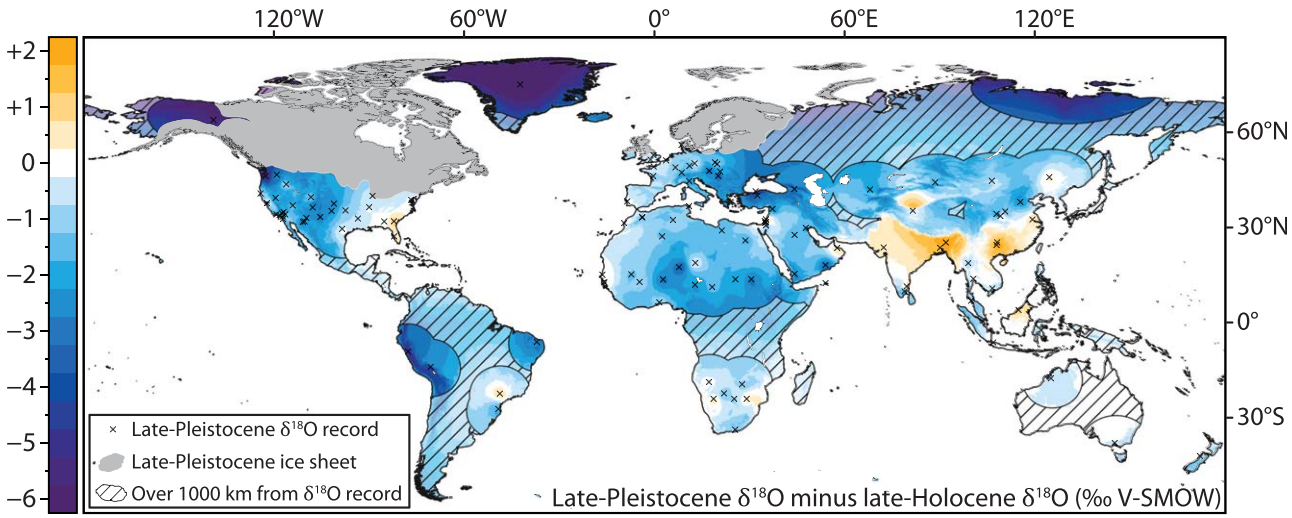

Figure 2. Interpolated late-Pleistocene minus late-Holocene precipitation δ^{18}O ($\Delta^{18}O_{\text{late-Pleistocene}}$). Measured $\Delta^{18}O_{\text{late-Pleistocene}}$ values are marked by cross symbols. Most terrestrial precipitation $\Delta^{18}O_{\text{late-Pleistocene}}$ values are negative (blue), meaning that late-Pleistocene precipitation was generally depleted in ^{18}O relative to the late-Holocene on the continents. Positive (orange) or near-zero $\Delta^{18}O_{\text{late-Pleistocene}}$ values are generally confined to the (sub)tropics (e.g., Florida, Senegal, Namibia, India, Bangladesh, southern China) and windward coasts (e.g., Maryland, Portugal).

3.1. Global Deglacial δ^{18}O Shifts

The global interpolation of $\Delta^{18}O_{\text{late-Pleistocene}}$ values demonstrates that late-Pleistocene precipitation δ^{18}O was lower than late-Holocene precipitation δ^{18}O over the great majority (~93%) of the global landmass (Figure 2). Spatial $\Delta^{18}O_{\text{late-Pleistocene}}$ patterns show that, broadly, tropical and subtropical $\Delta^{18}O_{\text{late-Pleistocene}}$ records have relatively low-magnitude $\Delta^{18}O_{\text{late-Pleistocene}}$ values that can be either positive or negative, whereas high-latitude records distal to coasts have negative $\Delta^{18}O_{\text{late-Pleistocene}}$ values (Figure 1). Positive $\Delta^{18}O_{\text{late-Pleistocene}}$ values are concentrated in warm humid climates influenced by the seasonal migration of the Intertropical Convergence Zone, including India, Bangladesh, south-central China, and Florida.

The 154 $\Delta^{18}O_{\text{late-Pleistocene}}$ records average −2.3‰, have a median of −1.3‰, a standard deviation of 3.0‰, an upper-lower quartile range of −3.2‰ to −0.4 ‰, and a 10th-90th percentile range of −6.6‰ to +0.4‰ (Figure 1). Tropical versus extratropical $\Delta^{18}O_{\text{late-Pleistocene}}$ values differ significantly from one another ($p < 0.0001$; two-tailed heteroscedastic *t*-test). Tropical record $\Delta^{18}O_{\text{late-Pleistocene}}$ values (within 25° of equator; n = 49) have a median of −0.9‰, an average of −1.5‰, a standard deviation of 2.2‰, an upper-lower quartile range of −2.7‰ to +0.1‰, and a 10th−90th percentile range of −4.7‰ to +0.8‰. Extratropical record $\Delta^{18}O_{\text{late-Pleistocene}}$ values (more than 35° from the equator; n = 70) have a median of −2.4‰, an average of −3.6‰, a standard deviation of 3.5‰, an upper-lower quartile range of −5.6‰ to −1.0‰, and a 10th–90th percentile range of −8.7‰ to −0.3‰.

Negative $\Delta^{18}O_{\text{late-Pleistocene}}$ values are common (128 of 154 records (82%)) in spite of the fact that evaporating seawater—the ultimate source of atmospheric moisture—was ~1‰ higher during the late-Pleistocene than during the late-Holocene [*Schrag et al.*, 1996]. Records of late-Pleistocene precipitation isotope compositions are scarce throughout Latin America, eastern Europe, central Asia, and equatorial Africa, but relatively common in the contiguous USA, southeast Asia, Europe, and northern and southern Africa (Figure 2; supporting information Figures S1 and S2).

Globally, high magnitude, negative $\Delta^{18}O_{\text{late-Pleistocene}}$ values coincide with sites that have low late-Holocene precipitation δ^{18}O values (Figure 3). Low modern precipitation δ^{18}O values characterize air masses that have lost large fractions of their original moisture contents to upwind rainout [*Dansgaard*, 1964]. Therefore, a plausible, first-order explanation for the global $\Delta^{18}O_{\text{late-Pleistocene}}$ trends is that the late-Pleistocene climate was characterized by stronger-than-modern isotopic distillation of advected air masses—that is, a higher-than-modern late-Pleistocene precipitation δ^{18}O gradient [*Jasechko et al.*, 2015]. Stronger-than-modern isotopic distillation during the late-Pleistocene is consistent with a nonlinear response of Rayleigh distillation to cooler glacial climate conditions, intensified further by the nonuniform glacial-interglacial warming that was largest outside the tropics and away from the coasts [*Annan and Hargreaves*, 2013]. However, the global

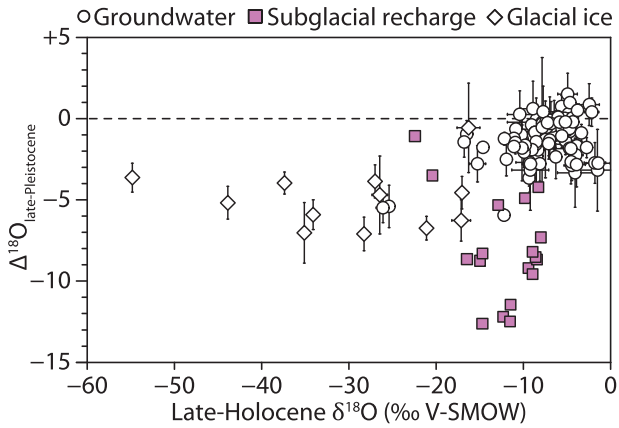

Figure 3. $\Delta^{18}O_{late\text{-}Pleistocene}$ and late-Holocene $\delta^{18}O$ values of groundwater (circles), glacial ice (diamonds), and subglacial recharge that occurred beneath the northern hemisphere ice sheets that existed over northern Europe and Canada during the last ice age (squares). Sites that have lower late-Holocene $\delta^{18}O$ values also have high magnitude, negative $\Delta^{18}O_{late\text{-}Pleistocene}$ values. The highest-magnitude, negative $\Delta^{18}O_{late\text{-}Pleistocene}$ values are records of paleoice sheet meltwaters recharged beneath the Laurentide and Fennoscandian ice sheets ("subglacial recharge"). Error bars mark ±1 standard deviation from the mean.

latitude-$\Delta^{18}O_{late\text{-}Pleistocene}$ relationship shown in Figure 1 is very likely impacted by numerous additional processes that have been previously highlighted as important drivers of precipitation $\delta^{18}O$ shifts between the Holocene and Pleistocene time periods. Some of the possible processes impacting the global latitude-$\Delta^{18}O_{late\text{-}Pleistocene}$ relationship include deglacial changes to global circulation patterns, sea surface temperatures, and moisture sources [e.g., *Rozanski*, 1985; *Hoffmann and Heimann*, 1997; *Sultan et al.*, 1997; *Aggarwal et al.*, 2004; *Cruz et al.*, 2006; *Tierney et al.*, 2008].

Zonally, late-Pleistocene $\delta^{18}O$ records located at latitudes of greater than 35° show near-uniform ^{18}O-depletion relative to the late-Holocene (77 of 78 extratropical sites). Conversely, only two-thirds of late-Pleistocene $\delta^{18}O$ records within 35° of the equator are ^{18}O-depleted relative to the late-Holocene (51 of 76 subtropical and tropical sites), while the remaining sites have positive $\Delta^{18}O_{late\text{-}Pleistocene}$ values (Figure 1a). Negative $\Delta^{18}O_{late\text{-}Pleistocene}$ values linked to the cool late-Pleistocene climate corroborate precipitation $\delta^{18}O$ estimates for the Eocene climate that simulate small modern-Eocene $\delta^{18}O$ changes across the low latitudes juxtaposed by higher magnitude, positive ($\delta^{18}O_{Eocene} > \delta^{18}O_{Modern}$) shifts closer to the poles [*Winnick et al.*, 2015]. Global hot (Eocene, [*Winnick et al.*, 2015]) and cold (late-Pleistocene, this study) house latitude-$\delta^{18}O$ gradients suggest that detectable impacts of modern climate warming driven by anthopogenic greenhouse gas emissions on precipitation $\delta^{18}O$ are likely to be maximized at the high latitudes rather than the equator.

Subglacial recharge records have the highest magnitude, negative $\Delta^{18}O_{late\text{-}Pleistocene}$ values in this data-synthesis (Figures 1 and 3). Subglacial records appear to have a distinct $\delta^{18}O_{late\text{-}Holocene}/\Delta^{18}O_{late\text{-}Pleistocene}$ isotopic relationship to that of direct, subaerial recharge (Figure 3). Specifically, some fossil groundwaters replenished beneath the Laurentide and Fennoscandian ice sheets have high-magnitude, negative $\Delta^{18}O_{late\text{-}Pleistocene}$ values (less than −7‰) and relatively high late-Holocene precipitation $\delta^{18}O$ values (about −15‰ to −8‰; see points for subglacial recharge in Figure 3). Differing $\delta^{18}O_{late\text{-}Holocene}/\Delta^{18}O_{late\text{-}Pleistocene}$ relationships of subaerially versus subglacially sourced paleowaters are plausibly due in part to the upstream englacial transport of ice that accumulated closer to topographic highs of the paleo ice sheets prior to subglacial recharge. $\delta^{18}O_{late\text{-}Holocene}/\Delta^{18}O_{late\text{-}Pleistocene}$ relationships may be used to distinguish two distinct recharge processes: (i) subaerial recharge from rain and melting snow, versus (ii) glacier-sourced recharge that took place underneath and along the peripheries of the large northern hemisphere ice sheets that existed during the Pleistocene ice ages.

3.2. Regional Deglacial $\delta^{18}O$ Shifts

High densities of $\Delta^{18}O_{late\text{-}Pleistocene}$ records are found across Africa, southeast Asia, and North America (Figure 4).

In northern Africa, high-magnitude and negative $\Delta^{18}O_{late\text{-}Pleistocene}$ values are found across western Niger, northern Nigeria, southern Chad, and southern Egypt (approximately −2 to −3‰). These continental $\Delta^{18}O_{late\text{-}Pleistocene}$ minima form a zonal band across central Africa between the subhumid Sudanian Savannah to the south and hyperarid Sahara to the north, indicating a zonal shift in regional hydroclimate between the late-Pleistocene and the late-Holocene along the modern Sahelian corridor. Relict sand dunes suggest the southern margin of the Sahara Desert was ~5° farther south than its present position at ~19°N during the late-Pleistocene [*Grove*, 1958]. Presence of a more southerly Sahara during the late-Pleistocene is

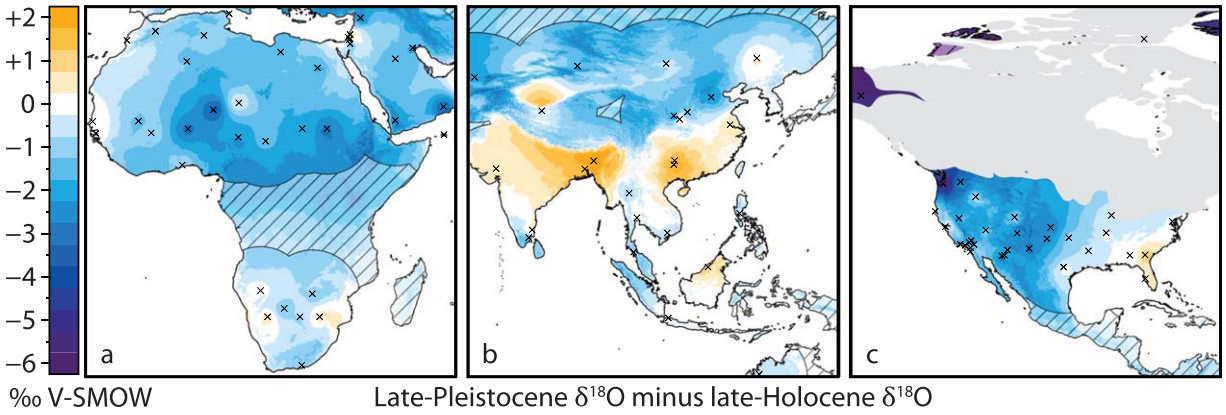

Figure 4. Interpolated late-Pleistocene minus late-Holocene precipitation δ^{18}O ($\Delta^{18}O_{late\text{-}Pleistocene}$) across (a) Africa, (b) southeast Asia, and (c) North America. Measured $\Delta^{18}O_{late\text{-}Pleistocene}$ values are marked by cross symbols. Most precipitation $\Delta^{18}O_{late\text{-}Pleistocene}$ values are negative, meaning that late-Pleistocene precipitation was generally depleted in ^{18}O relative to the late-Holocene on the continents. Gray shading in Figure 4c represents areas covered by ice during the late-Pleistocene.

further evidenced by dust abundances in offshore sediment cores that suggest the Sahara expanded south during late-Pleistocene Heinrich stadials [*Collins et al*., 2013]. Therefore, it is possible that the $\Delta^{18}O_{late\text{-}Pleistocene}$ minima along the modern Sahelian corridor are in part due to a deglacial shift in the Intertropical Convergence Zone from south (late-Pleistocene) to north (late-Holocene). However, the occurrence of the African Humid Period during the early Holocene—critically omitted from this data analysis and discussion because of the prescribed time intervals—provides strong evidence that nonlinear and complex hydroecological feedbacks linked to ocean circulation patterns and orbital precession are key drivers of African hydroclimate conditions [e.g., *Pokras and Mix*, 1985; *deMenocal et al*., 2000; *Gasse*, 2000; *Tjallingii et al*., 2008; *Tierney et al*., 2011]. Therefore, substantial fluctuations in African hydroclimate are not straightforwardly and solely linked to deglacial global warming, highlighting that detailed information about expansion-contraction cycles of the Sahara-Sahalian boundary are unlikely captured by the two-stage Pleistocene-to-Holocene precipitation δ^{18}O relationship calculated here.

In other regions of Africa, most $\Delta^{18}O_{late\text{-}Pleistocene}$ values are negative (Figure 4a; see also *Edmunds* [2009]). Near-zero $\Delta^{18}O_{late\text{-}Pleistocene}$ values are confined to coastlines such as west Morocco, Senegal, and Namibia. In southern Africa, western records have near-zero $\Delta^{18}O_{late\text{-}Pleistocene}$ values, whereas continental and southeastern records have negative $\Delta^{18}O_{late\text{-}Pleistocene}$ of moderate magnitudes (approximately $-1‰$). In equatorial Africa, few if any fossil groundwater $\Delta^{18}O_{late\text{-}Pleistocene}$ records are available, possibly highlighting a data gap that may be met by future field testing of groundwater systems located within $\sim 10°$ of the equator. However, leaf wax δ^2H records for east African rift lakes show large isotopic variations between the late-Pleistocene and the late-Holocene [*Tierney et al*., 2008]. These fluctuations occur at time scales of less than $\sim$5000 years and are therefore unlikely captured in full by fossil groundwater isotope records, highlighting the importance of other isotope proxy records that capture shifts at a relatively high temporal resolution (e.g., speleothems, ice cores, lake, and marine sediment cores).

In southeast Asia, $\Delta^{18}O_{late\text{-}Pleistocene}$ values are positive or near-zero throughout southcentral China, the Malay Archipelago, Bangladesh, and most of India (Figure 4b). Conversely, $\Delta^{18}O_{late\text{-}Pleistocene}$ values are consistently negative across northern China and along the Malay Peninsula. Near-zero and negative $\Delta^{18}O_{late\text{-}Pleistocene}$ values along the Malay Peninsula are located where two regional monsoon troughs converge [*Aggarwal et al*., 2004] and have lower $\Delta^{18}O_{late\text{-}Pleistocene}$ values than those observed to the west (Bangladesh), north (southern China), and east (Borneo), potentially impacted by different glacial-interglacial land-atmosphere feedbacks (e.g., moisture recycling by evaporation or plant transpiration) due to Pleistocene subaerial exposure of the Sunda Shelf [*Partin et al*., 2007].

In the contiguous USA, $\Delta^{18}O_{late\text{-}Pleistocene}$ values near to the southeastern coastline have near-zero and positive $\Delta^{18}O_{late\text{-}Pleistocene}$ values, whereas modern-day southwest deserts and central plains have consistently high magnitude, negative $\Delta^{18}O_{late\text{-}Pleistocene}$ values close to $-2.5‰$ [*Phillips et al*. 1986] (Figure 4c). Positive $\Delta^{18}O_{late\text{-}Pleistocene}$ values characterize hot humid climates along the southeast coast (e.g., Georgia and Florida) [*Plummer*, 1993; *Morrissey et al*., 2010], whereas $\Delta^{18}O_{late\text{-}Pleistocene}$ values along the southwest Pacific

coast are near-to-zero or negative (e.g., near Oakland, Los Angeles, San Diego in California). Continental-scale patterns of δ^{18}O are broadly similar for the late-Pleistocene and late-Holocene time periods, implying that the architecture of the largest, synoptic-scale moisture supplies to the contiguous USA may have remained broadly similar between the two climate states. However, $\Delta^{18}O_{\text{late-Pleistocene}}$ patterns show a steeper continental gradient in precipitation δ^{18}O during the late-Pleistocene relative to the late-Holocene, consistent with a nonlinear response of isotopic distillation that was plausibly intensified by larger glacial-interglacial temperature shifts distal to the coasts.

4. Concluding Remarks

The primary result of this study is a first estimate of the spatial distribution of deglacial precipitation δ^{18}O shifts across the global landmass (Figure 2). The global map of deglacial precipitation δ^{18}O shifts suggests (i) that extratropical precipitation was near-uniformly ^{18}O-depleted relative to the late-Holocene, (ii) that subtropical and tropical precipitation δ^{18}O responses to deglacial climate warming diverge between the two monsoonal climates of Africa and southest Asia, (iii) that groundwaters recharged by meltwaters of the Fennoscandian and Laurentide ice sheets might be distinguished from subaerial-sourced paleogroundwaters on the basis of their δ^{18}O values, (iv) that late-Pleistocene precipitation at the great majority of high latitudes and high altitudes was strongly ^{18}O-depleted relative to the late-Holocene, and (v) that polar air masses likely underwent stronger-than-modern isotopic distillation as they advected poleward during the late-Pleistocene.

Broader implications of late-Pleistocene precipitation δ^{18}O maps could extend to a number of different fields, as evidenced by the array of applications of modern precipitation δ^{18}O maps to mammal migration and ecosystem water use studies. It is therefore possible that late-Pleistocene precipitation δ^{18}O distributions, while of poor temporal resolution, could provide some constraints on certain late-Pleistocene earth and biologic systems processes. For example, late-Pleistocene paleowater δ^{18}O values have in past been used to distinguish palaeogroundwaters from younger Holocene-aged groundwaters, thereby better constraining groundwater velocity and mixing [*Samborska et al.*, 2012]. The maps developed here show that the usefulness of δ^{18}O measurements to partition groundwater age distributions (i.e., fractions of Holocene and paleogroundwater in a sample) is likely to be greatest in regions with high magnitude $\Delta^{18}O_{\text{late-Pleistocene}}$ values (e.g., north Africa, continental North America, east Europe, central Asia). Further, the interpolated $\Delta^{18}O_{\text{late-Pleistocene}}$ data could help provide data-driven constraints on Pleistocene/Holocene spatial precipitation δ^{18}O gradients that have been used in past to reconstruct and constrain Pleistocene mammal migration extents [e.g., *Koch et al.*, 1998]. Finally, the $\Delta^{18}O_{\text{late-Pleistocene}}$ maps developed here may help to evaluate the numerous isotope-enabled climate models that are applied frequently to evaluate hypotheses about glacial climate dynamics and the impacts of deglacial climate warming on water resources.

Acknowledgments
I thank G. Ferguson, A. Lechler, F. S. R. Pausata, P. J. Fawcett, T. Gleeson, D. I. Cendón, J. Galewsky, A. N. LeGrande, C. Risi, Z. D. Sharp, J. M. Welker, M. Werner, and K. Yoshimura for discussions while writing two previously published paleowater papers. I am grateful to two anonymous reviewers for their helpful comments that improved this work. The International Atomic Energy Agency (IAEA) and the US Geological Survey (USGS) are acknowledged for supporting development of many of the groundwater isotope records analyzed in this study and thanked for making these data freely available for the community. The analyzed data were downloaded from online databases (USGS and IAEA) or were compiled from the primary literature (citations shown in supporting information Table S1 and in the caption of Figure 1). This work was supported by **NSERC Discovery** grant **5668**.

References

Abbott, M. D., A. Lini, and P. R. Bierman (2000), δ^{18}O, δD and ^{3}H measurements constrain groundwater recharge patterns in an upland fractured bedrock aquifer, Vermont, USA, *J. Hydrol.*, *228*, 101–112.

Aeschbach-Hertig, W., M. Stute, J. F. Clark, R. F. Reuter, and P. Schlosser, (2002), A paleotemperature record derived from dissolved noble gases in groundwater of the Aquia Aquifer (Maryland, USA), *Geochim. Cosmochim. Acta*, *66*, 797–817.

Aggarwal, P. K., et al. (2000), Isotope hydrology of groundwater in Bangladesh: Implications for characterization and mitigation of arsenic in groundwater, IAEA-TC Proj. Rep. BGD/8/016, 65 pp., International At. Energy Agency, Vienna.

Aggarwal, P. K., K. Fröhlich, K. M. Kulkarni, and L. L. Gourcy, (2004), Stable isotope evidence for moisture sources in the Asian summer monsoon under present and past climate regimes, *Geophys. Res. Lett.*, *31*, L08203, *doi*:10.1029/2004GL019911.

Airey, P. L., G. E. Calf, P. E. Hartley, and D. Roman (1980), Aspects of the isotope hydrology of two sandstone aquifers in arid Australia, in *Arid-zone Hydrology: Investigations with Isotope Techniques*, pp. 93–111, International At. Energy Agency, Vienna.

Al-Mashaikhi, K., S. Oswald, S. Attinger, G. Büchel, K. Knöller, and G. Strauch (2012), Evaluation of groundwater dynamics and quality in the Najd aquifers located in the Sultanate of Oman, *Environ. Earth Sci.*, *66*, 1195–1211.

Al-Ruwaih, F. M., and M. Shehata (2004), Hydrochemical processes and environmental isotopic study of groundwater in Kuwait, *Water Int.*, *29*, 158–166.

Andrews, J. N., J-Ch. Fontes, J.-F. Aranyossy, A. Dodo, W. M. Edmunds, A. Joseph, and Y. Travi (1994), The evolution of alkaline groundwaters in the continental intercalaire aquifer of the Irhazer Plain, Niger, *Water Resour. Res.*, *30*, 45–61.

Annan, J. D., and J. C. Hargreaves (2013), A new global reconstruction of temperature changes at the Last Glacial Maximum, *Clim. Past*, *9*, 367–376.

Aravena, R., and L. I. Wassenaar (1993), Dissolved organic carbon and methane in a regional confined aquifer, southern Ontario, Canada: Carbon isotope evidence for associated subsurface sources, *Appl. Geochem.*, *8*, 483–493.

Asmerom, Y., V. J. Polyak, and S. J. Burns (2010), Variable winter moisture in the southwestern United States linked to rapid glacial climate shifts, *Nat. Geosci.*, *3*, 114–117.

Bar-Matthews, M., A. Ayalon, and A. Kaufman (1997), Late Quaternary paleoclimate in the eastern Mediterranean region from stable isotope analysis of speleothems at Soreq Cave, Israel, *Quat. Res.*, *47*, 155–168.

Bar-Matthews, M., A. Ayalon, M. Gilmour, A. Matthews, and C. Hawkesworth, (2003), Sea-land oxygen isotopic relationships from planktonic foraminifera and speleothems in the Eastern Mediterranean region and their implication for paleorainfall during interglacial intervals, *Geochim. Cosmochim. Acta*, *67*, 3181–3199.

Barbecot, F., C. Marlin, E. Gibert, and L. Dever (2000), Hydrochemical and isotopic characterisation of the Bathonian and Bajocian coastal aquifer of the Caen area (northern France), *Appl. Geochem.*, *15*, 791–805.

Berkelhammer, M., A. Sinha, L. Stott, H. Cheng, F. S. R. Pausata, and K. Yoshimura, (2012), An abrupt shift in the Indian monsoon 4000 years ago, in *Climates, Landscapes, and Civilizations*, edited by L. D. Q. Giosan et al., AG U, Washington, D. C.

Beyerle, U., R. Purtschert, W. Aeschbach-Hertig, D. M. Imboden, H. H. Loosli, R. Wieler, and R. Kipfer (1998), Climate and groundwater recharge during the last glaciation in an ice-covered region. *Science*, *282*, 731–734.

Beyerle, U., J. Rueedi, M. Leuenberger, W. Aeschbach-Hertig, F. Peeters, R. Kipfer, and A. Dodo, (2003), Evidence for periods of wetter and cooler climate in the Sahel between 6 and 40 kyr BP derived from groundwater, *Geophys. Res. Lett.*, *30*(4), 1173, doi:10.1029/2002GL016310.

Blunier, T., and E. J. Brook (2001), Timing of millennial-scale climate change in Antarctica and Greenland during the last glacial period, *Science*, *291*, 109–112.

Bowen, G. J., and B. Wilkinson (2002), Spatial distribution of δ^{18}O in meteoric precipitation, *Geology*, *30*, 315–318.

Brown, K. B., J. C. McIntosh, L. K. Rademacher, and K. A. Lohse (2011), Impacts of agricultural irrigation recharge on groundwater quality in a basalt aquifer system (Washington, USA): A multi-tracer approach, *Hydrogeol. J.*, *19*, 1039–1051.

Buiron, D., et al. (2011), TALDICE-1 age scale of the Talos Dome deep ice core, East Antarctica, *Clim. Past*, *7*, 1–16.

Cai, Y., L. Tan, H. Cheng, Z. An, R. L. M. J. Edwards, Kelly, X. Kong, and X. Wang (2010), The variation of summer monsoon precipitation in central China since the last deglaciation, *Earth Planet. Sci. Lett.*, *291*, 21–31.

Cartwright, I., T. R. Weaver, D. I. Cendón, L. K. Fifield, S. O. Tweed, B. Petrides, and I. Swane (2012), Constraining groundwater flow, residence times, inter-aquifer mixing, and aquifer properties using environmental isotopes in the southeast Murray Basin, Australia, *Appl. Geochem.*, *27*, 1698–1709.

Castany, G., A. Marce, J. Margat, H. Moussu, Y. Vuillaume, and J. Evin (1974), An environmental isotope study of the groundwater regime in large aquifers, in *Isotope Techniques in Groundwater Hydrology 1974*, vol. I., pp. 243–256, International At. Energy Agency, Vienna, Austria.

Celle-Jeanton, H. F. Huneau, Y. Travi, and W. M. Edmunds, (2009), Twenty years of groundwater evolution in the Triassic sandstone aquifer of Lorraine: Impacts on baseline water quality, *Appl. Geochem.*, *24*, 1198–1213.

Chen, Z., Z. Nie, Z. Zhang, J. Qi, and Y. Nan (2005), Isotopes and sustainability of ground water resources, North China Plain, *Groundwater*, *43*, 485–493.

Chen, Z., W. Wei, J. Liu, Y. Wang, and J. Chen (2011), Identifying the recharge sources and age of groundwater in the Songnen Plain (Northeast China) using environmental isotopes, *Hydrogeol. J.*, *19*, 163–176.

Cheung, K., and B. Mayer (2009), Chemical and Isotopic Characterization of Shallow Groundwater from Selected Monitoring Wells in Alberta: 2006-2007, Alberta environment report, Alberta Environment, Edmonton, Canada, 88 pp.

Clark, I. D., and P. Fritz (1997), *Environmental Isotopes in Hydrogeology*, CRC Press, Boca Raton, Fla.

Clark, I. D., P. Fritz, O. P. Quinn, P. W. Rippon, H. Nash, and S. B. B. G. al Said (1987), Modern and fossil groundwater in an arid environment: A look at the hydrogeology of southern Oman, in *Isotope Techniques in Water Resources Development*, pp. 167–187, International At. Energy Agency, Vienna, Austria.

Clark, I. D., M. Douglas, K. Raven, and D. Bottomley (2000), Recharge and preservation of Laurentide glacial melt water in the Canadian Shield, *Groundwater*, *38*, 735–742.

Clark, J. F., M. Stute, P. Schlosser, S. Drenkard, and G. Bonani (1997), A tracer study of the Floridan aquifer in southeastern Georgia: Implications for groundwater flow and paleoclimate, *Water Resour. Res.*, *33*, 281–289.

Clark, J. F., M. L. Davisson, G. B. Hudson, and P. A. Macfarlane (1998), Noble gases, stable isotopes, and radiocarbon as tracers of flow in the Dakota aquifer, Colorado and Kansas, *J. Hydrol.*, *211*, 151–167.

Clark, P. U., et al. (2009), The last glacial maximum, *Science*, *325*, 710–714.

Cody, J. D., I. E. Hutcheon, and H. R. Krouse (1999), Fluid flow, mixing and the origin of CO_2 and H_2S by bacterial sulphate reduction in the Mannville Group, southern Alberta, Canada, *Mar. Pet. Geol.*, *16*, 495–510.

Collins, J. A., A. Govin, S. Mulitza, D. Heslop, M. Zabel, J. Hartmann, U. Röhl, and G. Wefer, (2013), Abrupt shifts of the Sahara–Sahel boundary during Heinrich stadials, *Clim. Past*, *9*, 1181–1191.

Cruz, F. W., S. J. Burns, I. Karmann, W. D. Sharp, M. Vuille, A. O. Cardoso, J. A. Ferrari, P. L. S. Dias, and O. Viana (2005), Insolation-driven changes in atmospheric circulation over the past 116,000 years in subtropical Brazil, *Nature*, *434*, 63–66.

Cruz, F. W., S. J. Burns, I. Karmann, W. D. Sharp, and M. Vuille (2006), Reconstruction of regional atmospheric circulation features during the late Pleistocene in subtropical Brazil from oxygen isotope composition of speleothems, *Earth Planet. Sci. Lett.*, *248*, 495–507.

Currell, M., D. I. Cendon, and X. Cheng (2013), Analysis of environmental isotopes in groundwater to understand the response of a vulnerable coastal aquifer to pumping: Western Port Basin, south-eastern Australia, *Hydrogeol. J.*, *21*, 1413–1427.

Currell, M. J., I. Cartwright, D. C. Bradley, and D. Han (2010), Recharge history and controls on groundwater quality in the Yuncheng Basin, north China, *J. Hydrol.*, *385*, 216–229.

Cuthbert, M. O., et al. (2014), Evaporative cooling of speleothem drip water, *Sci. Rep.*, *4*, 1–7, 5162, doi:10.1038/srep05162.

Dansgaard, W. (1964), Stable isotopes in precipitation, *Tellus Ser. A*, *16*, 436–468.

Dansgaard, W., et al. (1993), Evidence for general instability of past climate from a 250-kyr ice-core record, *Nature*, *364*, 218–220.

Darling, W. G., W. M. Edmunds, and P. L. Smedley (1997), Isotopic evidence for palaeowaters in the British Isles, *Appl. Geochem.*, *12*, 813–829.

Datta, P. S., S. K. Bhattacharya, and S. K. Tyagi (1996), ^{18}O studies on recharge of phreatic aquifers and groundwater flow-paths of mixing in the Delhi area, *J. Hydrol.*, *176*, 25–36.

Deininger, M., J. Fohlmeister, D. Scholz, and A. Mangini (2012), Isotope disequilibrium effects: The influence of evaporation and ventilation effects on the carbon and oxygen isotope composition of speleothems: A model approach, *Geochim. Cosmochim. Acta*, *96*, 57–79.

deMenocal, P., J. Ortiz, T. Guilderson, J. Adkins, M. Sarnthein, L. Baker, and M. Yarusinsky (2000), Abrupt onset and termination of the African Humid Period: Rapid climate responses to gradual insolation forcing, *Quat. Sci. Rev.*, *19*, 347–361.

Derwich, L. J., K. Zouar, and J. L. Michelot (2012), Recharge and paleorecharge of the deep groundwater aquifer system in the Zeroud Basin (Kairouan plain, Central Tunisia), *Quat. Int.*, *257*, 56–63.

Dodo, A., and G. M. Zuppi (1997), Étude des écoulements souterrains dans le bassin de Bilma-Djado ā l'aide des isotopes de l'environnement, *C. R. Acad. Sci. Ser. II*, *325*, 845–852.

Dodo, A., and G. M. Zuppi (1999), Variabilité climatique durant le Quaternaire dans la nappe du Tarat (Arlit, Niger), *C. R. Acad. Sci. Ser. II*, *328*, 371–379.

Douglas, A., J. L. Osiensky, and C. K. Keller (2007), Carbon-14 dating of ground water in the Palouse Basin of the Columbia river basalts, *J. Hydrol.*, *334*, 502–512.

Dutt, S., A. K. Gupta, S. C. Clemens, H. Cheng, R. K. Singh, G. Kathayat, and R. L. Edwards (2015), Abrupt changes in Indian summer monsoon strength during 33,800 to 5500 years B.P., *Geophys. Res. Lett.*, *42*, 5526–5532, doi:10.1002/2015GL064015.

Dutton, A. R. (1995), Groundwater isotopic evidence for paleorecharge in US High Plains aquifers, *Quat. Res.*, *43*, 221–231.

Dykoski, C. A., R. L. Edwards, H. Cheng, D. Yuan, Y. Cai, M. Zhang, Y. Lin, J. Qing, Z. An, and J. Revenaugh (2005), A high-resolution, absolute-dated Holocene and deglacial Asian monsoon record from Dongge Cave, China, *Earth Planet. Sci. Lett.*, *233*, 71–86.

Eberts, S. M., and L. L. George (2000), Regional ground-water flow and geochemistry in the Midwestern basins and arches aquifer system in parts of Indiana, Ohio, Michigan, and Illinois, *U.S. Geol. Surv. Prof. Pap.*, *1423-C*, 103 pp.

Edmunds, W. M. (2009), Palaeoclimate and groundwater evolution in Africa: Implications for adaptation and management, *Hydrol. Sci. J.*, *54*, 781–792.

Edmunds, W. M., and E. P. Wright (1979), Groundwater recharge and palaeoclimate in the Sirte and Kufra basins, Libya, *J. Hydrol.*, *40*, 215–241.

Edmunds, W. M., A. H. Guendouz, A. Mamou, A. Moulla, P. Shand, and K. Zouari (2003), Groundwater evolution in the Continental Intercalaire aquifer of southern Algeria and Tunisia: Trace element and isotopic indicators, *Appl. Geochem.*, *18*, 805–822.

Edmunds, W. M., A. Dodo, D. Djoret, F. Gasse, C. B. Gaye, I. B. Goni, Y. Travi, K. Zouari, and G. M. Zuppi, (2004), Groundwater as an archive of climatic and environmental change, in *Past Climate Variability Through Europe and Africa, Dev. Palaeoenviron. Res. Ser.*, edited by R. W. Battarbee, F. Gasse, and C. E. Stickley, pp. 279–306, Springer Verlag, Dordrecht, Netherlands.

Elliot, T., J. N. Andrews, and W. M. Edmunds (1999), Hydrochemical trends, palaeorecharge and groundwater ages in the fissured Chalk aquifer of the London and Berkshire Basins, UK, *Appl. Geochem.*, *14*, 333–363.

EPICA Community (2006), One-to-one coupling of glacial climate variability in Greenland and Antarctica, *Nature*, *444*, 195–198.

Fadlelmawla, A., K. Hadi, K. Zouari, and K. M. Kulkarni (2008), Hydrogeochemical investigations of recharge and subsequent salinization processes at Al-Raudhatain depression in Kuwait, *Hydrol. Sci. J.*, *53*, 204–223.

Feng, X., A. M. Faiia, and E. S. Posmentier, (2009), Seasonality of isotopes in precipitation: A global perspective, *J. Geophys. Res.*, *114*, D08116, doi:10.1029/2008JD011279.

Ferguson, G. and S. Jasechko, (2015), The isotopic composition of the Laurentide Ice Sheet and fossil groundwater, *Geophys. Res. Lett.*, *42*, 4856–4861, doi:10.1002/2015GL064106.

Ferguson, G. A., R. N. Betcher, and S. E. Grasby (2007), Hydrogeology of the Winnipeg formation in Manitoba, Canada, *Hydrogeol. J.*, *15*, 573–587.

Fernandes, P. G., and P. M. Carreira (2008), Isotopic evidence of aquifer recharge during the last ice age in Portugal, *J. Hydrol.*, *361*, 291–308.

Ferronsky, V. I., V. A. Polyakov, and S. V. Ferronsky (1991), Isotope variations in the hydrological cycle as a tool in a climate change mechanism study, in *Isotope Techniques in Water Resources Development*, pp. 567–586, International At. Energy Agency, Vienna, Austria.

Fleitmann, D., et al. (2009), Timing and climatic impact of Greenland interstadials recorded in stalagmites from northern Turkey, *Geophys. Res. Lett.*, *36*, L19707, doi:10.1029/2009GL040050.

Florea, L. J. (2013), Selective recharge and isotopic composition of shallow groundwater within temperate, epigenic carbonate aquifers, *J. Hydrol.*, *489*, 201–213.

Frumkin, A., D. C. Ford, and H. P. Schwarcz (1999), Continental oxygen isotopic record of the last 170,000 years in Jerusalem, *Quat. Res.*, *51*, 317–327.

Gasse, F. (2000), Hydrological changes in the African tropics since the Last Glacial Maximum, *Quat. Sci. Rev.*, *19*, 189–211.

Gat, J. R. (1996), Oxygen and hydrogen isotopes in the hydrologic cycle, *Annu. Rev. Earth Planet. Sci.*, *24*, 225–262.

Gat, J. R., and A. Galai (1982), Groundwaters of the Arava Valley: An isotopic study of their origin and interrelationships, *Isr. J. Earth Sci.*, *31*, 25–38.

Geyh, M. A., and B. Sofner, (1989), Groundwater analysis of environmental carbon and other isotopes from the Jakarta Basin Aquifer, Indonesia, *Radiocarbon*, *31*, 919–925.

Gonfiantini, R., T. Dincer, and A. M. Derekoy (1974), Environmental isotope hydrology in the Hodna region, Algeria, in *Isotope Techniques in Groundwater Hydrology 1974*, vol. I., pp. 293–314, International At. Energy Agency, Vienna, Austria.

Goni, I. B. (2006), Tracing stable isotope values from meteoric water to groundwater in the southwestern part of the Chad basin, *Hydrogeol. J.*, *14*, 742–752.

Gosselin, D. C., F. E. Harvey, C. Frost, R. Stotler, and P. A. Macfarlane (2004), Strontium isotope geochemistry of groundwater in the central part of the Dakota (Great Plains) aquifer, USA, *Appl. Geochem.*, *19*, 359–377.

Gouvea da Silva, R. B. (1983), Estudo hidroquımico e isotópico das águas subterrâneas do aquıfero Botucatu no estado de Sao Paulo, PhD thesis, Univ. of Sao Paulo, Sao Paulo, Brazil.

Grabczak, J., K. Rozanski, P. Maloszewski, and A. Zuber, (1984), Estimation of the tritium input function with the aid of stable isotopes, *Catena*, *11*, 105–114.

Grasby, S. E., and R. N. Betcher (2002), Regional hydrogeochemistry of the carbonate rock aquifer, southern Manitoba, *Can. J. Earth Sci.*, *39*, 1053–1063.

Grasby, S. E., and Z. Chen (2005), Subglacial recharge into the Western Canada Sedimentary Basin—Impact of Pleistocene glaciation on basin hydrodynamics, *Geol. Soc. Am. Bull.*, *117*, 500–514.

Grasby, S. E., C. C. Allen, T. G. Longazo, J. T. Lisle, D. W. Griffin, and B. Beauchamp, (2003), Supraglacial sulfur springs and associated biological activity in the Canadian high arctic-signs of life beneath the ice, *Astrobiology*, *3*, 583–596.

Greene, S., N. Battye, I. Clark, T. Kotzer, and D. Bottomley, (2008), Canadian Shield brine from the Con Mine, Yellowknife, NT, Canada: Noble gas evidence for an evaporated Palaeozoic seawater origin mixed with glacial meltwater and Holocene recharge, *Geochim. Cosmochim. Acta*, *72*, 4008–4019.

Grootes, P. M., and M. Stuiver (1997), Oxygen $^{18}O/^{16}O$ variability in Greenland snow and ice with 10^{-3}- to 10^{5}-year time resolution, *J. Geophys. Res.*, *102*, 26,455–26,470.

Grove, A. T. (1958), The ancient erg of Hausaland, and similar formations on the south side of the Sahara, *Geogr. J.*, *124*, 528–533.
Hackley, K. C., S. V. Panno, and T. F. Anderson, (2010), Chemical and isotopic indicators of groundwater evolution in the basal sands of a buried bedrock valley in the midwestern United States: Implications for recharge, rock-water interactions, and mixing, *Geol. Soc. Am. Bull.*, *122*, 1047–1066.
Hagedorn, B. (2015), Hydrochemical and ^{14}C constraints on groundwater recharge and interbasin flow in an arid watershed: Tule Desert, Nevada, *J. Hydrol.*, *523*, 297–308.
Harrington, G., L. Stelfox, P. Gardner, P. Davies, R. Doble, and P. Cook, (2011), Surface Water – Groundwater Interactions in the Lower Fitzroy River, Western Australia, CSIRO report, 54 pp., Water for a Healthy Country Natl. Res. Flagship.
Harrison, S. P., P. J. Bartlein, K. Izumi, G. Li, J. Annan, J. Hargreaves, P. Braconnot, and M. Kageyama (2015), Evaluation of CMIP5 palaeosimulations to improve climate projections, *Nat. Clim. Change*, *5*, 735–743.
Heaton, T. H. E., A. S. Talma, and J. C. Vogel, (1986), Dissolved gas paleotemperatures and 18O variations derived from groundwater near Uitenhage, South Africa, *Quat. Res.*, *25*, 79–88.
Hendry, M. J., and L. I. Wassenaar (2009), Inferring heterogeneity in aquitards using high-resolution δD and δ^{18}O profiles, *Ground Water*, *47*, 639–645.
Hendry, M. J., S. L. Barbour, K. Novakowski, and L. I. Wassenaar, (2013), Paleohydrogeology of the Cretaceous sediments of the Williston Basin using stable isotopes of water, *Water Resour. Res.*, *49*, 4580–4592, doi:10.1002/wrcr.20321.
Hinsby, K., W. G. Harrar, P. Nyegaard, P. B. Konradi, E. S. Rasmussen, T. Bidstrup, U. Gregersen, and E. Boaretto, (2001), The Ribe Formation in western Denmark: Holocene and Pleistocene groundwaters in a coastal Miocene sand aquifer, *Geol. Soc. Spec. Publ.*, *189*, 29–48.
Hoaglund, J. R., J. J. Kolak, D. T. Long, and G. J. Larson (2004), Analysis of modern and Pleistocene hydrologic exchange between Saginaw Bay (Lake Huron) and the Saginaw Lowlands area, *Geol. Soc. Am. Bull.*, *116*, 3–15.
Hoffmann, G., and M. Heimann (1997), Water isotope modeling in the Asian monsoon region, *Quat. Int.*, *37*, 115–128.
Holmgren, K., J. A. Lee-Thorp, G. R. Cooper, K. Lundblad, T. C. Partridge, L. Scott, R. Sithaldeen, A. S. Talma, and P. D. Tyson, (2003), Persistent millennial-scale climatic variability over the past 25,000 years in Southern Africa, *Quat. Sci. Rev.*, *22*, 2311–2326.
Hoque, M. A., and W. G. Burgess (2012), ^{14}C dating of deep groundwater in the Bengal Aquifer System, Bangladesh: Implications for aquifer anisotropy, recharge sources and sustainability, *J. Hydrol.*, *444*, 209–220.
Huneau, F., D. Dakoure, H. Celle-Jeanton, T. Vitvar, M. Ito, S. Traore, N. F. Compaore, H. Jirakova, and P. Le Coustumer (2011), Flow pattern and residence time of groundwater within the south-eastern Taoudeni sedimentary basin (Burkina Faso, Mali), *J. Hydrol.*, *409*, 423–439.
Jasechko, S. (2016), Partitioning young and old groundwater with geochemical tracers, *Chem. Geol.*, *427*, 35–42.
Jasechko, S., and R. G. Taylor (2015), Intensive rainfall recharges tropical groundwaters, *Environ. Res. Lett.*, *10*, 124015.
Jasechko, S., et al. (2014), The pronounced seasonality of global groundwater recharge, *Water Resour. Res.*, *50*, 8845–8867, doi:10.1002/2014WR015809.
Jasechko, S., et al. (2015), Late glacial to late Holocene shifts in global precipitation δ^{18}O, *Clim. Past*, *11*, 1375–1393.
Jones, I. C., and J. L. Banner (2003), Estimating recharge thresholds in tropical karst island aquifers: Barbados, Puerto Rico and Guam, *J. Hydrol.*, *278*, 131–143.
Karro, E., A. Marandi, and R. Vaikmäe (2004), The origin of increased salinity in the Cambrian-Vendian aquifer system on the Kopli Peninsula, northern Estonia, *Hydrogeol. J.*, *12*, 424–435.
Kawamura, K., et al. (2007), Northern Hemisphere forcing of climatic cycles in Antarctica over the past 360,000 years, *Nature*, *448*, 912–916.
Klump, S., T. Grundl, R. Purtschert, and R. Kipfer (2008), Groundwater and climate dynamics derived from noble gas, ^{14}C, and stable isotope data, *Geology*, *36*, 395–398.
Koch, P. L., K. A. Hoppe, and S. D. Webb (1998), The isotopic ecology of late Pleistocene mammals in North America: Part 1. Florida, *Chem. Geol.*, *152*, 119–138.
Kolak, J. J., D. T. Long, J. M. Matty, G. J. Larson, D. F. Sibley, and T. B. Councell, (1999), Ground-water, large-lake interactions in Saginaw Bay, Lake Huron: A geochemical and isotopic approach, *Geol. Soc. Am. Bull.*, *111*, 177–188.
Kotler, E., and C. R. Burn (2000), Cryostratigraphy of the Klondike "muck" deposits, west central Yukon Territory, *Can. J. Earth Sci.*, *37*, 849–861.
Kreuzer, A. M., C. von Rohden, R. Friedrich, Z. Chen, J. Shi, I. Hajdas, R. Kipfer, and W. Aeschbach-Hertig (2009), A record of temperature and monsoon intensity over the past 40 kyr from groundwater in the North China Plain, *Chem. Geol.*, *259*, 168–180.
Külls, C. (2000), Groundwater of the North-Western Kalahari, Namibia: Estimation of recharge and quantification of the flow systems, PhD dissertation, 230 pp. Univ. of Würzburg, Würzburg, Germany.
Kulongoski, J. T., D. R. Hilton, and E. T. Selaolo (2004), Climate variability in the Botswana Kalahari from the late Pleistocene to the present day, *Geophys. Res. Lett.*, *31*, L10204, doi:10.1029/2003GL019238.
Kulongoski, J. T., D. R. Hilton, R. G. Cresswell, S. Hostetler, and G. Jacobson (2008), Helium-4 characteristics of groundwaters from Central Australia: Comparative chronology with chlorine-36 and carbon-14 dating techniques, *J. Hydrol.*, *348*, 176–194.
Kumar, U. S., S. Sharma, S. V. Navada, and A. S. Deodhar (2009), Environmental isotopes investigation on recharge processes and hydrodynamics of the coastal sedimentary aquifers of Tiruvadanai, Tamilnadu State, India, *J. Hydrol.*, *364*, 23–39.
Larsen, F., R. Owen, T. Dahlin, P. Mangeya, and G. Barmen, (2002), A preliminary analysis of the groundwater recharge to the Karoo formations, mid-Zambezi basin, Zimbabwe, *Phys. Chem. Earth*, *27*, 765–772.
Le Gal La Salle, C., C. Marlin, S. Savoye, and J.-F. Fontes, (1995), Geochemistry and ^{14}C dating of groundwaters from Jurassic aquifers of North Aquitaine Basin (France), *Appl. Geochem.*, *11*, 433–445.
Le Gal La Salle, C., C. Marlin, C. Leduc, J. D. Taupin, M. Massault, and G. Favreau, (2001), Renewal rate estimation of groundwater based on radioactive tracers (^{3}H, ^{14}C) in an unconfined aquifer in a semi-arid area, Iullemeden Basin, Niger, *J. Hydrol.*, *254*, 145–156.
Lee, J.-E., K. Johnson, and I. Fung (2009), Precipitation over South America during the Last Glacial Maximum: An analysis of the "amount effect" with a water isotope-enabled general circulation model, *Geophys. Res. Lett.*, *36*, L19701, doi:10.1029/2009GL039265.
Li, J., Z. Pang, K. Froehlich, T. Huang, Y. Kong, W. Song, and H. Yun (2015), Paleo-environment from isotopes and hydrochemistry of groundwater in East Junggar Basin, Northwest China, *J. Hydrol.*, *529*, 650–661.
Majumder, R. K., M. A. Halim, B. B. Saha, R. Ikawa, T. Nakamura, M. Kagabu, and J. Shimada, (2011), Groundwater flow system in Bengal Delta, Bangladesh revealed by environmental isotopes, *Environ. Earth Sci.*, *64*, 1343–1352.
Marcott, S. A., J. D. Shakun, P. U. Clark, and A. C. Mix, (2013), A reconstruction of regional and global temperature for the past 11,300 years, *Science*, *339*, 1198–1201.
Martinelli, G., A. Chahoud, A. Dadomo, and A. Fava, (2014), Isotopic features of Emilia-Romagna region (North Italy) groundwaters: Environmental and climatological implications, *J. Hydrol.*, *519*, 1928–1938.
Maulé, C. P., D. S. Chanasyk, and K. Muehlenbachs (1994), Isotopic determination of snow-water contribution to soil water and groundwater, *J. Hydrol.*, *155*, 73–91.

Mazor, E., D. Gilad, and V. Fridman, (1995), Stagnant aquifer concept Part 2: Small scale artesian systems: Hazeva, Dead Sea Rift Valley, Israel, *J. Hydrol.*, *173*, 241–261.
McMahon, P. B., J. K. Böhlke, and S. C. Christenson (2004), Geochemistry, radiocarbon ages, and paleorecharge conditions along a transect in the central High Plains aquifer, southwestern Kansas, USA, *Appl. Geochem.*, *19*, 1655–1686.
Mehta, S., A. E. Fryar, and J. L. Banner (2000), Controls on the regional-scale salinization of the Ogallala aquifer, Southern High Plains, Texas, USA, *Appl. Geochem.*, *15*, 849–864.
Melikadze, G., N. Zhukova, M. Todadze, S. Vepkhvadze, N. Kapanadze, A. Chankvetadze, T. Jimsheladze, and T. Vitvar, (2014), Evaluation of recharge origin of groundwater in the Alazani-Iori basins, using hydrochemical and isotope approaches, *J. Georg. Geophys. Soc.*, *17a*, 53–64.
Meyer, H., A. Y. Derevyagin, C. Siegert, and H. W. Hubberten (2002), Paleoclimate studies on Bykovsky Peninsula, North Siberia-hydrogen and oxygen isotopes in ground ice, *Polarforschung*, *70*, 37–51.
Mickler, P. J., L. A. Stern, and J. L. Banner (2006), Large kinetic isotope effects in modern speleothems, *Geol. Soc. Am. Bull.*, *118*, 65–81.
Mix, H. T., and C. P. Chamberlain (2014), Stable isotope records of hydrologic change and paleotemperature from smectite in Cenozoic western North America, *Geochim. Cosmochim. Acta*, *141*, 532–546.
Morrissey, S. K., J. F. Clark, M. Bennett, E. Richardson, and M. Stute (2010), Groundwater reorganization in the Floridan aquifer following Holocene sea-level rise, *Nat. Geosci.*, *3*, 683–687.
Naus, C. A., D. G. Driscoll, and J. M. Carter (2001), Geochemistry of the Madison and Minnelusa aquifers in the Black Hills area, South Dakota, *U.S. Geol. Surv. Water Resour. Invest. Rep.*, *01-4129*, 118.
New, M., D. Lister, M. Hulme, and I. Makin (2002), A high-resolution data set of surface climate over global land areas, *Clim. Res.*, *21*, 1–25.
Noseck, U., K. Rozanski, M. Dulinski, V. Havlová, O. Sracek, T. Brasser, M. Hercik, and G. Buckau (2009), Carbon chemistry and groundwater dynamics at natural analogue site Ruprechtov, Czech Republic: Insights from environmental isotopes, *Appl. Geochem.*, *24*, 1765–1776.
O'Driscoll, M. A., D. R. DeWalle, K. J. McGuire, and W. J. Gburek, (2005), Seasonal ^{18}O variations and groundwater recharge for three landscape types in central Pennsylvania, *USA, J. Hydrol.*, *303*, 108–124.
O'Neil, J. R., R. N. Clayton, and T. K. Mayeda, (1969), Oxygen isotope fractionation in divalent metal carbonates, *J. Chem. Phys.*, *51*, 5547–5558.
Partin, J. W., K. M. Cobb, J. F. Adkins, B. Clark, and D. P. Fernandez (2007), Millennial-scale trends in west Pacific warm pool hydrology since the Last Glacial Maximum, *Nature*, *449*, 452–455.
Patterson, L. J., et al. (2005), Cosmogenic, radiogenic, and stable isotopic constraints on groundwater residence time in the Nubian Aquifer, Western Desert of Egypt, *Geochem. Geophys. Geosyst.*, *6*, Q01005, doi:10.1029/2004GC000779.
Patterson, W. S. B., R. M. Koerner, D. Fisher, S. J. Johnsen, H. B. Clausen, W. Dansgaard, P. Bucher, and H. Oeschger, (1977), An oxygen-isotope climatic record from the Devon Island ice cap, arctic Canada, *Nature*, 266, 508−511.
Pausata, F. S. R., D. S. Battisti, K. H. Nisancioglu, and C. M. Bitz (2011), Chinese stalagmite δ^{18}O controlled by changes in the Indian monsoon during a simulated Heinrich event, *Nat. Geosci.*, *4*, 474–480.
Pedro, J. B., T. D. Van Ommen, S. O. Rasmussen, V. I. Morgan, J. Chappellaz, A. D. Moy, V. Masson-Delmotte, and M. Delmotte (2011), The last deglaciation: Timing the bipolar seesaw, *Clim. Past*, *7*, 671–683.
Person, M., J. McIntosh, V. Bense, and V. H. Remenda, (2007), Pleistocene hydrology of North America: The role of ice sheets in reorganizing groundwater flow systems, *Rev. Geophys.*, *45*, RG3007, doi:10.1029/2006RG000206.
Phillips, F. M., L. A. Peeters, M. K. Tansey, and S. N. Davis (1986), Paleoclimatic inferences from an isotopic investigation of groundwater in the central San Juan Basin, New Mexico, *Quat. Res.*, *26*, 179–193.
Plummer, L. N. (1993), Stable isotope enrichment in paleowaters of the southeast Atlantic Coastal Plain, United States, *Science*, *262*, 2016–2020.
Pokras, E. M., and A. C. Mix (1985), Eolian evidence for spatial variability of late Quaternary climates in tropical Africa, *Quat. Res.*, *24*, 137–149.
Rahube, T. B. (2003), Recharge and groundwater resources evaluation of the Lokalane-Ncojane basin (Botswana) using numerical modelling, thesis, 119 pp., Int. Inst. for Geo-inform. Sci. and Earth Observ, Enschede, Netherlands.
Raidla, V., K. Kirsimäe, R. Vaikmäe, A. Jõeleht, E. Karro, A. Marandi, and L. Savitskaja, (2009), Geochemical evolution of groundwater in the Cambrian–Vendian aquifer system of the Baltic Basin, *Chem. Geol.*, *258*, 219–231.
Raidla, V., K. Kirsimäe, R. Vaikmäe, E. Kaup, and T. Martma, (2012), Carbon isotope systematics of the Cambrian–Vendian aquifer system in the northern Baltic Basin: Implications to the age and evolution of groundwater, *Appl. Geochem.*, *27*, 2042–2052.
Remenda, V. H., J. A. Cherry, and T. W. D. Edwards (1994), Isotopic composition of old ground water from Lake Agassiz: Implications for late Pleistocene climate, *Science*, *266*, 1975–1978.
Remenda, V. H., G. van der Kamp, and J. A. Cherry (1996), Use of vertical profiles of δ^{18}O to constrain estimates of hydraulic conductivity in a thick, unfractured aquitard, *Water Resour. Res.*, *32*, 2979–2987.
Risi, C., D. Noone, C. Frankenberg, and J. Worden, (2013), Role of continental recycling in intraseasonal variations of continental moisture as deduced from model simulations and water vapor isotopic measurements, *Water Resour. Res.*, *49*, 4136–4156, doi:10.1002/wrcr.20312.
Rozanski, K. (1985), Deuterium and oxygen-18 in European groundwaters—links to atmospheric circulation in the past, *Chem. Geol.*, *52*, 349–363.
Rozanski, K., L. Araguás-Araguás, and R. Gonfiantini (1993), Isotopic patterns in modern global precipitation, in Climate Change in Continental Isotopic Records, AGU, 1–36.
Salati, E., A. Dall'Olio, E. Matsui, and J. R. Gat, (1979), Recycling of water in the Amazon basin: An isotopic study, *Water Resour. Res.*, *15*, 1250–1258.
Salati, E., J. Menezes Leal, and M. Mendes Campos (1974), Environmental isotopes used in a hydrogeological study of northeastern Brazil, in *Isotope Techniques in Groundwater Hydrology*, vol. I., pp. 379–398, Int. Atomic Energy Agency, Vienna, Austria.
Samborska, K., A. Różkowski, and P. Małoszewski (2012), Estimation of groundwater residence time using environmental radioisotopes (^{14}C, T) in carbonate aquifers, southern Poland, *Isot. Environ. Health Stud.*, *49*, 73–97.
Sánchez-Murillo, R., and C. Birkel (2016), Groundwater recharge mechanisms inferred from isoscapes in a complex tropical mountainous region, *Geophys. Res. Lett.*, *43*, 5060–5069, doi:10.1002/2016GL068888.
Schlegel, M. E., A. L. Mayo, S. Nelson, D. Tingey, R. Henderson, and D. Eggett, (2009), Paleo-climate of the Boise area, Idaho from the last glacial maximum to the present based on groundwater δ^2H and δ^{18}O compositions, *Quat. Res.*, *71*, 172–180.
Schrag, D. P., G. Hampt, and D. W. Murray (1996), Pore fluid constraints on the temperature and oxygen isotopic composition of the glacial ocean, *Science*, *272*, 1930–1932.

Schwartz, F. W., and K. Muehlenbachs (1979), Isotope and ion geochemistry of groundwaters in the Milk River aquifer, Alberta, *Water Resour. Res.*, *15*, 259–268.

Shakun, J. D., S. J. Burns, D. Fleitmann, J. Kramers, A. Matter, and A. Al-Subary (2007), A high-resolution, absolute-dated deglacial speleothem record of Indian Ocean climate from Socotra Island, Yemen, *Earth Planet. Sci. Lett.*, *259*, 442–456.

Shehata, M., and F. Al-Ruwaih (1999), Major ions geochemistry and environmental isotope study of the Nubian Aquifer system, Dakhla Oasis, Western Desert, Egypt, *Arab. J. Sci. Eng.*, *24*, 43–58.

Siegel, D. I., and R. J. Mandle (1984), Isotopic evidence for glacial meltwater recharge to the Cambrian-Ordovician aquifer, north-central United States, *Quat. Res.*, *22*, 328–335.

Sikdar, P. K., and P. Sahu (2009), Understanding wetland sub-surface hydrology using geologic and isotopic signatures, *Hydrol. Earth Syst. Sci.*, *13*, 1313–1323.

Simpson, E. S., D. B. Thorud, and I. Friedman (1972), Distinguishing seasonal recharge to groundwater by deuterium analysis in southern Arizona, in Proceedings of the Reeding Symposium, pp. 113–121, Int. Assoc. of Sci. Hydrol.

Stadler, S., M. A. Geyh, D. Ploethner, and P. Koeniger (2012), The deep Cretaceous aquifer in the Aleppo and Steppe basins of Syria: Assessment of the meteoric origin and geographic source of the groundwater, *Hydrogeol. J.*, *20*, 1007–1026.

Steen-Larsen, H. C., et al. (2014), What controls the isotopic composition of Greenland surface snow?, *Clim. Past*, *10*, 377–392.

Stotler, R. L., S. K. Frape, T. Ruskeeniemi, L. Ahonen, T. C. Onstott, and M. Y. Hobbs, (2009), Hydrogeochemistry of groundwaters in and below the base of thick permafrost at Lupin, Nunavut, Canada. *J. Hydrol.*, *373*, 80–95.

Stotler, R. L., S. K. Frape, and O. Shouakar-Stash (2010), An isotopic survey of δ^{81}Br and δ^{37}Cl of dissolved halides in the Canadian and Fennoscandian Shields, *Chem. Geol.*, *274*, 38–55.

Stute, M., and J. Deák (1989), Environmental isotope study ^{14}C, ^{13}C, ^{18}O, D, noble gases on deep groundwater circulation systems in Hungary with reference to paleoclimate, *Radiocarbon*, *31*, 902–918.

Sukhija, B. S., D. V. Reddy, and P. Nagabhushanam (1998), Isotopic fingerprints of paleoclimates during the last 30,000 years in deep confined groundwaters of Southern India, *Quat. Res.*, *50*, 252–260.

Sultan, M., N. Sturchio, F. A. Hassan, M. A. R. Hamdan, A. M. Mahmood, Z. El Alfy, and T. Stein (1997), Precipitation source inferred from stable isotopic composition of Pleistocene groundwater and carbonate deposits in the Western desert of Egypt, *Quat. Res.*, *48*, 29–37.

Sultan, M., E. Yan, N. Sturchio, A. Wagdy, K. Abdel Gelil, R. Becker, N. N. Manocha, and A. Milewski, (2007), Natural discharge: A key to sustainable utilization of fossil groundwater, *J. Hydrol.*, *335*, 25−35.

Taylor, R. G., et al. (2013a), Ground water and climate change, *Nat. Clim. Change*, *3*, 322–329.

Taylor, R. G., M. C. Todd, L. Kongola, L. Maurice, E. Nahozya, H. Sanga, and A. M. MacDonald, (2013b), Evidence of the dependence of groundwater resources on extreme rainfall in East Africa, *Nat. Clim. Change*, *3*, 374–378.

Tenu, A., P. Noto, G. Cortecci, and S. Nuti (1975), Environmental isotopic study of the Barremian-Jurassic aquifer in south Dobrogea (Roumania), *J. Hydrol.*, *26*, 185–198.

Thompson, L. G., E. Mosley-Thompson, M. E. Davis, J. F. Bolzan, J. Dai, L. Klein, T. Yao, X. Wu, Z. Xie, and N. Gundestrup, (1989), Holocene-late Pleistocene climatic ice core records from Qinghai-Tibetan Plateau, *Science*, *246*, 474–477.

Thompson, L. G., E. Mosley-Thompson, M. E. Davis, P. N. Lin, K. A. Henderson, J. Cole-Dai, J. F. Bolzan, and K. B. Liu (1995), Late glacial stage and Holocene tropical ice core records from Huascaran, Peru, *Science*, *269*, 46–50.

Thompson, L. G., T. Yao, M. E. Davis, K. A. Henderson, E. Mosley-Thompson, P. N. Lin, J. Beer, H.-A. Synal, J. Cole-Dai, and J. F. Bolzan (1997), Tropical climate instability: The last glacial cycle from a Qinghai-Tibetan ice core, *Science*, *276*, 1821–1825.

Thompson, L. G., et al. (1998), A 25,000-year tropical climate history from Bolivian ice cores, *Science*, *282*, 1858–1864.

Tierney, J. E., J. M. Russell, Y. Huang, J. S. S. Damsté, E. C. Hopmans, and A. S. Cohen, (2008), Northern hemisphere controls on tropical southeast African climate during the past 60,000 years, *Science*, *322*, 252–255.

Tierney, J. E., S. C. Lewis, B. I. Cook, A. N. LeGrande, and G. A. Schmidt, (2011), Model, proxy and isotopic perspectives on the East African Humid Period, *Earth Planet. Sci. Lett.*, *307*, 103–112.

Tjallingii, R., M. Claussen, J. B. W. Stuut, J. Fohlmeister, A. Jahn, T. Bickert, F. Lamy, and U. Röhl (2008), Coherent high-and low-latitude control of the northwest African hydrological balance, *Nat. Geosci.*, *1*, 670–675.

Torgersen, T., R. Purtschert, F. M. Phillips, L. N. Plummer, W. E. Sanford, and A. Suckow, (2013), Defining groundwater age, in *Isotope Methods for Dating Old Groundwater*, International At. Energy Agency, Vienna, Austria.

Turney, C. S. M., et al. (2015), Obliquity-driven expansion of North Atlantic sea ice during the last glacial, *Geophys. Res. Lett.*, *42*, 10,382–10,390, doi:10.1002/2015GL066344.

van Geldern, R., A. Baier, H. L. Subert, S. Kowol, L. Balk, and J. A. C. Barth, (2014), Pleistocene paleo-groundwater as a pristine fresh water resource in southern Germany: Evidence from stable and radiogenic isotopes, *Sci. Total Environ.*, *496*, 107–115.

Varsányi, I., L. Palcsu, and L. Ó. Kovács (2011), Groundwater flow system as an archive of palaeotemperature: Noble gas, radiocarbon, stable isotope and geochemical study in the Pannonian Basin, Hungary, *Appl. Geochem.*, *26*, 91–104.

Vinther, B. M., et al. (2006), A synchronized dating of three Greenland ice cores throughout the Holocene, *J. Geophys. Res.*, *111*, D13102, doi:10.1029/2005JD006921.

Vinther, B. M., H. B. Clausen, D. A. Fisher, R. M. Koerner, S. J. Johnsen, K. K. Andersen, D. Dahl-Jensen, S. O. Rasmussen, J. P. Steffensen, and A. M. Svensson, (2008), Synchronizing ice cores from the Renland and Agassiz ice caps to the Greenland Ice Core Chronology, *J. Geophys. Res.*, *113*, D08115, doi:10.1029/2007JD009143.

Vogel, J. C., D. Ehhalt, and W. Roether (1963), A survey of the natural isotopes of water in South Africa, in *Proceedings of Tokyo Conference on Radioisotopes in Hydrology*, International Atomic Energy Agency, Vienna, Austria, pp. 407–416.

von Rohden, C., A. Kreuzer, Z. Chen, R. Kipfer, and W. Aeschbach-Hertig (2010), Characterizing the recharge regime of the strongly exploited aquifers of the North China Plain by environmental tracers, *Water Resour. Res.*, *46*, W05511, *doi*:10.1029/2008WR007660.

Wagner, J. D. M., J. E. Cole, J. W. Beck, P. J. Patchett, G. M. Henderson, and H. R. Barnett, (2010), Moisture variability in the southwestern United States linked to abrupt glacial climate change, *Nat. Geosci.*, *3*, 110–113.

Walraevens, K. (1990), Natural isotope research on groundwater from the semi-confined Ledo-Paniselian aquifer in Belgium: Application of ^{14}C-correction methods, *Nat. Tijdsehr*, *72*, 79–89.

Wang, X. F., et al. (2007), Millennial-scale precipitation changes in southern Brazil over the past 90,000 years, *Geophys. Res. Lett.*, *34*, L23701, doi:10.1029/2007GL031149.

Wang, Y. J., H. Cheng, R. L. Edwards, Z. S. An, J. Y. Wu, C. C. Shen, and J. A. Dorale, (2001), A high-resolution absolute-dated late Pleistocene monsoon record from Hulu Cave, China, *Science*, *294*, 2345–2348.

Weaver, T. R., S. K. Frape, and J. A. Cherry (1995), Recent cross-formational fluid flow and mixing in the shallow Michigan Basin, *Geol. Soc. Am. Bull.*, *107*, 697–707.

Weyhenmeyer, C. E., S. J. Burns, H. N. Waber, W. Aeschbach-Hertig, R. Kipfer, H. H. Loosli, and A. Matter, (2000), Cool glacial temperatures and changes in moisture source recorded in Oman groundwaters, *Science*, *287*, 842–845.

Weyhenmeyer, C. E., S. J. Burns, H. N. Waber, P. G. Macumber, and A. Matter, (2002), Isotope study of moisture sources, recharge areas, and groundwater flow paths within the eastern Batinah coastal plain, Sultanate of Oman, *Water Resour. Res.*, *38*(10), 1184, doi:10.1029/2000WR000149.

Wieser, M., W. Aeschbach-Hertig, T. Schneider, R. D. Deshpande, and S. K. Gupta, (2011), A temperature and monsoon record derived from environmental tracers in the groundwater of northwest India. in *Isotopes in Hydrology, Marine Ecosystems and Climate Change Studies*, vol. I., pp. 7–14, International At. Energy Agency, Vienna, Austria.

Williams, J. J. W. (2009), Quaternary vegetation distribution, in *Encyclopedia of Paleoclimatology and Ancient Environments*, edited by V. Gornitz, pp. 856–861, Springer, N. Y.

Williams, P. W., H. L. Neil, and J. X. Zhao (2010), Age frequency distribution and revised stable isotope curves for New Zealand speleothems: Palaeoclimatic implications, *Int. J. Speleol.*, *39*, 99–112.

Winnick, M. J., C. P. Chamberlain, J. K. Caves, and J. M. Welker (2014), Quantifying the isotopic 'continental effect,' *Earth Planet. Sci. Lett.*, *406*, 123–133.

Winnick, M. J., J. K. Caves, and C. P. Chamberlain (2015), A mechanistic analysis of early Eocene latitudinal gradients of isotopes in precipitation, *Geophys. Res. Lett.*, *42*, 8216–8224, doi:10.1002/2015GL064829.

Winograd, I. J., A. C. Riggs, and T. B. Coplen, (1998), The relative contributions of summer and cool-season precipitation to groundwater recharge, Spring Mountains, Nevada, USA. *Hydrogeol. J.*, *6*, 77–93.

Yang, Y., D. Yuan, H. Cheng, M. Zhang, J. Qin, Y. Lin, Z. XiaoYan, and R. L. Edwards (2010), Precise dating of abrupt shifts in the Asian monsoon during the last deglaciation based on stalagmite data from Yamen Cave, Guizhou Province, China, *Sci. China Earth Sci.*, *53*, 633–641.

Yechieli, Y., U. Kafri, and O. Sivan (2008), The inter-relationship between coastal sub-aquifers and the Mediterranean Sea, deduced from radioactive isotopes analysis, *Hydrogeol. J.*, *17*, 264–274.

Yuan, D., et al. (2004), Timing, duration, and transitions of the last interglacial Asian monsoon, *Science*, *23*, 575–578.

Zuber, A., S. M. Weise, J. Motyka, K. Osenbrück, and K. Różański (2004), Age and flow pattern of groundwater in a Jurassic limestone aquifer and related Tertiary sands derived from combined isotope, noble gas and chemical data, *J. Hydrol.*, *286*, 87–112.